The Astrophysical Journal, 735:106 (21pp), 2011 July 10 doi:10.1088/0004-637X/735/2/106

THE DISCOVERY AND NATURE OF THE OPTICAL TRANSIENT CSS100217:102913+404220*,†

A. J. Drake[1], S. G. Djorgovski[1], A. Mahabal[1], J. Anderson[2], R. Roy[3], V. Mohan[4], S. Ravindranath[4], D. Frail[5], S. Gezari[6], James D. Neill[1], L. C. Ho[7], J. L. Prieto[7], D. Thompson[8], J. Thorstensen[9], M. Wagner[8], R. Kowalski[10], J. Chiang[11], J. E. Grove[12], F. K. Schinzel[13], D. L. Wood[12], L. Carrasco[14], E. Recillas[14], L. Kewley[15], K. N. Archana[16,17], Aritra Basu[17], Yogesh Wadadekar[17], Brijesh Kumar[3], A. D. Myers[18], E. S. Phinney[1], R. Williams[1], M. J. Graham[1], M. Catelan[19], E. Beshore[10], S. Larson[10], and E. Christensen[20]

[1] California Institute of Technology, 1200 E. California Blvd., CA 91225, USA
[2] STScI, 3700 San Martin Drive, Baltimore, MD 21218, USA
[3] Aryabhatta Research Institute of Observational Sciences, Manora Peak, Nainital 263129, Uttarakhand, India
[4] IUCAA, Postbag 4, Ganeshkhind, Pune 411007, India
[5] NRAO, Campus Building 65, 949 North Cherry Avenue, Tucson, AZ 85721-0655, USA
[6] Department of Physics & Astronomy, Johns Hopkins University, 366 Bloomberg Center, 3400 N. Charles Street, Baltimore, MD 21218, USA
[7] Carnegie Observatories, 813 Santa Barbara Street, Pasadena, CA 91101, USA
[8] LBT, University of Arizona, 933 N. Cherry Ave, Room 552, Tucson, AZ 85721, USA
[9] Dartmouth College, 6127 Wilder Laboratory, Hanover, NH 03755-3528, USA
[10] Department of Planetary Sciences, Lunar and Planetary Laboratory, The University of Arizona, 1629 E. University Blvd., Tucson, AZ 85721, USA
[11] W. W. Hansen Experimental Physics Laboratory, Kavli Institute for Particle Astrophysics and Cosmology, SLAC National Accelerator Laboratory, Stanford University, Standford, CA 94305, USA
[12] Space Science Division, Naval Research Laboratory, Washington, DC 20375, USA
[13] Max-Planck-Institut für Radioastronomie, Auf dem Hügel 69, 53121 Bonn, Germany
[14] INAOE, Tonantzintla, Puebla, Mexico
[15] IFA, 640 North A'ohoku Place, #209, Hilo, HI 96720-2700, USA
[16] School of Computer Sciences, Mahatma Gandhi University, Kottayam 686560, India
[17] National Centre for Radio Astrophysics, TIFR, Post Bag 3, Ganeshkhind, Pune 411007, India
[18] Department of Astronomy, University of Illinois at Urbana-Champaign, Urbana, IL 61801, USA
[19] Departamento de Astronomía y Astrofísica, Pontificia Universidad Católica de Chile, Av. Vicuña Mackena 4860, 782-0436 Macul, Santiago, Chile
[20] Gemini Observatory, Casilla 603, La Serena, CL, Chile
Received 2010 December 17; accepted 2011 April 26; published 2011 June 22

ABSTRACT

We report on the discovery and observations of the extremely luminous optical transient CSS100217:102913+404220 (CSS100217 hereafter). Spectroscopic observations showed that this transient was coincident with a galaxy at redshift $z = 0.147$ and reached an apparent magnitude of $V \sim 16.3$. After correcting for foreground Galactic extinction we determine the absolute magnitude to be $M_V = -22.7$ approximately 45 days after maximum light. Over a period of 287 rest-frame days, this event had an integrated bolometric luminosity of 1.3×10^{52} erg based on time-averaged bolometric corrections of ∼15 from *V*- and *R*-band observations. Analysis of the pre-outburst Sloan Digital Sky Survey (SDSS) spectrum of the source shows features consistent with a narrow-line Seyfert 1 galaxy. High-resolution *Hubble Space Telescope* and Keck follow-up observations show that the event occurred within 150 pc of the nucleus of the galaxy, suggesting a possible link to the active nuclear region. However, the rapid outburst along with photometric and spectroscopic evolution are much more consistent with a luminous supernova. Line diagnostics suggest that the host galaxy is undergoing significant star formation. We use extensive follow-up of the event along with archival Catalina Sky Survey NEO search and SDSS data to investigate the three most likely sources of such an event: (1) an extremely luminous supernova, (2) the tidal disruption of a star by the massive nuclear black hole, and (3) variability of the central active galactic nucleus (AGN). We find that CSS100217 was likely an extremely luminous Type IIn supernova and occurred within the range of the narrow-line region of an AGN. We discuss how similar events may have been missed in past supernova surveys because of confusion with AGN activity.

Key words: galaxies: active – galaxies: nuclei – galaxies: stellar content – supernovae: general

Online-only material: color figures

1. INTRODUCTION

Exploration of the time domain is now one of the most rapidly growing and exciting areas of astrophysics. This vibrant observational frontier has fueled the advent of the new generation of digital synoptic sky surveys, which cover the sky many times, as well as the necessity of using robotic telescopes to respond rapidly to transient events (Paczynski 2000). However, the discovery of transient astronomical events is by no means new to astronomy with phenomena such as supernovae being discovered and documented for centuries (Zhao et al. 2006). Transient events themselves have been observed on timescales from seconds; e.g., gamma-ray bursts (GRBs; Klebesadel et al. 1973), to years; e.g., supernovae (Rest et al. 2011) and active galactic nuclei (AGNs; Ulrich et al. 1997). Predictions of new types of observable astrophysical phenomena continue to be theorized

* Some of the data presented herein were obtained at the W. M. Keck Observatory, which is operated as a scientific partnership among the California Institute of Technology, the University of California, and the National Aeronautics and Space Administration. The Observatory was made possible by the generous financial support of the W. M. Keck Foundation.
† Based on observations made with the NASA/ESA *Hubble Space Telescope*, obtained at the Space Telescope Science Institute, which is operated by the Association of Universities for Research in Astronomy, Inc., under NASA contract NAS 5-26555. These observations are associated with program 12117.

and made detectable by advancing technology. For example, the possibility that Massive Compact Halo Objects could be observable due to gravitational microlensing was theorized by Paczynski (1986) and soon proven by Alcock et al. (2003) and Aubourg et al. (1993). Such discoveries set the stage for larger time domain surveys with broader goals.

A systematic exploration of the observable parameter space in the time domain is very likely to lead to many new discoveries (e.g., Djorgovski et al. 2001a, 2001b, and references therein). For example, many types of transient events have been theoretically predicted, yet remain to be convincingly observed. Among these are GRB orphan afterglows (Nakar et al. 2002) and the electromagnetic counterparts to gravitational-wave inspiral events, where close binaries coalesce to release a surge of gravitational radiation (Abadie et al. 2010). Nevertheless, the recent detections of rare types of transients, including candidate pair-instability supernovae (Gal-Yam et al. 2010), tidal disruption events (TDEs; Gezari et al. 2009a; van Velzen et al. 2010), and supernova shock breakouts (Soderberg et al. 2008; Schawinski et al. 2008) show the promise of current and future large transient surveys.

Recent optical surveys searching for transient phenomena include ROTSE (Akerlof et al. 2000), Sloan Digital Sky Survey (SDSS; Sesar et al. 2007), Palomar Quest (PQ; Djorgovski et al. 2008), the Catalina Real-time Transient Survey (CRTS; Drake et al. 2009), Palomar Transient Factory (PTF; Rau et al. 2009), and the Panoramic Survey Telescope & Rapid Response System (PanSTARRS; Hodapp et al. 2004). In the near future additional surveys such as SkyMapper (Keller et al. 2007) and the Large Synoptic Survey Telescope (LSST; Ivezic et al. 2008) will begin operation. At radio wavelengths work is being undertaken by the low-frequency array (Rottgering 2003), the Allen Telescope Array (Croft et al. 2009) and will soon begin with the Australian Square Kilometre Array Pathfinder (Johnston et al. 2007). At high energies ongoing satellite searches for transients include the *Fermi* Large Area Telescope (LAT; Atwood et al. 2009), *Swift* (Barthelmy et al. 2005), and *Galaxy Evolution Explorer* (*GALEX*; Martin et al. 2005), *Rossi X-ray Timing Explorer* (Jahoda et al. 1996), and the Monitor of All-sky X-ray Image (Ueno et al. 2008).

As the temporal and spatial coverage of transient surveys increases, there are prospects for the discovery of rare events on short timescales. To this end, the new generation of transient surveys are increasingly working on real-time analysis and detection. In late 2007, the CRTS (Drake et al. 2009) simultaneously began real-time analysis and notification of events in images taken by the Catalina Sky Survey NEO search (CSS; Larson et al. 2003). The CRTS transient survey currently analyzes data from three telescopes operated by CSS. These telescopes cover $\sim$1800 deg^2 on the sky per night to a depth ranging from $V = 19$ to 21.5. New objects are automatically flagged in real time and filtered to isolate genuine optical transients from artifacts and other noise sources. In order to maximize discovery potential all CRTS transients are immediately distributed publicly as VO-Events.[21] For each of the few dozen transient events detected per night a portfolio of historical observational information is extracted from past surveys from radio to gamma-ray wavelengths. This information allows most events to be classified into a few broad types of phenomena including supernovae, blazars, and cataclysmic variable outbursts. Objects which are of uncertain nature are examined in greater detail using Virtual Observatory services such as DataScope.[22] Events that remain a poor match for known types phenomena are of particular interest and are the most closely scrutinized.

2. THE DISCOVERY OF CSS100217

On 2010 February 17 we discovered the transient event CSS100217 during the course of the CRTS. This event was flagged as unusual at discovery as the object had a past spectrum from the SDSS (Abazajian et al. 2009) that resembled a Seyfert, yet the outburst was uncharacteristically rapid and large for an AGN. Additionally, there was no detection in archival FIRST and NRAO VLA Sky Survey (NVSS) radio data covering the object's location. The lack of any radio source suggests that the variability was not being powered by a jet, as seen with optically variable blazars. Given the unexpected nature of the event, we immediately scheduled photometric and spectroscopic follow-up of the event.

3. MULTI-WAVELENGTH OBSERVATIONS

Following the discovery of the clearly energetic event we undertook follow-up observations in X-ray, UV, optical, near-IR, and radio wavelengths as well as a targeted archival gamma-ray search. In Table 1, we present the sequence and nature of the follow-up observations we obtained. In the following section we will discuss the details of each set of observations as well as historical data for the source galaxy. We will then combine the data to interpret the nature of the event in relation to known types of transients and make concluding remarks about the source.

3.1. UV, Optical, and Near-IR Photometry

Following CSS100217's discovery, unfiltered observations continued as part of the CSS survey. All CSS photometry is routinely transformed to *V*-magnitudes by using between 10 and 100 G-type dwarf calibration stars measured in each 8 deg^2 image. These calibration stars are pre-selected using Two Micron All Sky Survey (2MASS) near-IR data.[23] The magnitudes for each calibration star are transformed to *V* following Bessell & Brett (1988), and the zero point for each field is derived. The scatter in the *V* magnitude for the calibration stars is typically $<$0.05 mag (Larson et al. 2003). To improve the quality of the photometry for CSS100217 we created a high signal-to-noise ratio (S/N) template image and carried out image subtraction (Tomaney & Crotts 1996) on all the CSS images. This process reduces the photometric dependence on external calibrators, but can introduce uncertainty due to the subtraction process. Based on our analysis the zero-point uncertainty is approximately 0.1 mag.

In Figure 1, we present the CSS light curve of the transient plus host galaxy flux determined from the template image. In order to determine the brightness of the transient we carried out image subtraction (Tomaney & Crotts 1996) on the CSS data using a combined high signal-to-noise template image produced from observations taken before the outburst. The flux of the transient source is thus in units of the template image flux. We determine the brightness of the transient by calibrating the flux using the magnitudes of stars measured in the template image. CSS photometry is available in Table 2. SDSS photometric observations taken in late 2002 and early 2003 exhibit *r* and *i* magnitudes of 17.6 and 17.3, respectively, and is given in

[21] http://crts.caltech.edu/ and SkyAlert, http://www.skyalert.org/.

[22] http://heasarc.gsfc.nasa.gov/cgi-bin/vo/datascope/init.pl

[23] http://www.ipac.caltech.edu/2mass/releases/allsky/doc/explsup.html

Table 1
Observation Sequence

Telescope + Instrument	Passbands	Observation Date (YYYY-MM-DD)
Photometry	Filters	
SDSS	*u*, *g*, *r*, *i*, *z*	2002-12-31 × 2, 2003-03-26
CSS + 4K CDD	*V* (unfiltered)	2003–2010
ARIES 1 m	*U*, *B*, *V*, *R*, *I*	2010-04+
Palomar 1.5 m	*g*, *r*, *i*, *z*	2010-03-02, 2010-03-11, 2010-06-22, 2010-06-23
SWIFT + UVOT	*UVW1, UVM2, UVW2, U, B, V*	2010-04-06, 2010-04-25, 2010-05-09, 2010-05-23
GALEX	NUV, FUV	2004-01-24, 2010-01-29, 2010-04-17, 2010-04-29
HST + WFC3	F390W, F555W, F763M	2010-05-31
Keck + AO	NIR	2010-06-02
LBT + LUCIFER	K_s	2010-05-02
GHO 2.1 m +CANICA	*J*, *H*, K_s	2010-04+
Spectra	Wavelength Range (Å)	
SDSS + MOS	3800–9100	2002-12-29
IGO + IFOSC	4000–8600	2010-02-18, 2010-04-04, 2010-04-23
P200 + DBSP	3500–9100	2010-03-15, 2010-11-09
APO + DIS	3500–9600	2010-04-09
GALEX + NUV grism	1900–2800	2010-04-17, 2010-04-29
MDM 2.4 m + Modspec	4200–7560	2010-05-04
Keck-I + LRIS	3100–10100	2010-05-18
Radio	Central Frequency	
EVLA	4.5 GHz + 7.9 GHz	2010-04-29, 2010-05-14, 2010-06-01
GMRT	608 mHz	2010-05-23
X-ray and γ-ray	Energy	
Swift +XRT	0.2–10 keV	2010-04-06
Fermi +LAT	20 MeV–300 GeV	2009-11-20 to 2010-07-04

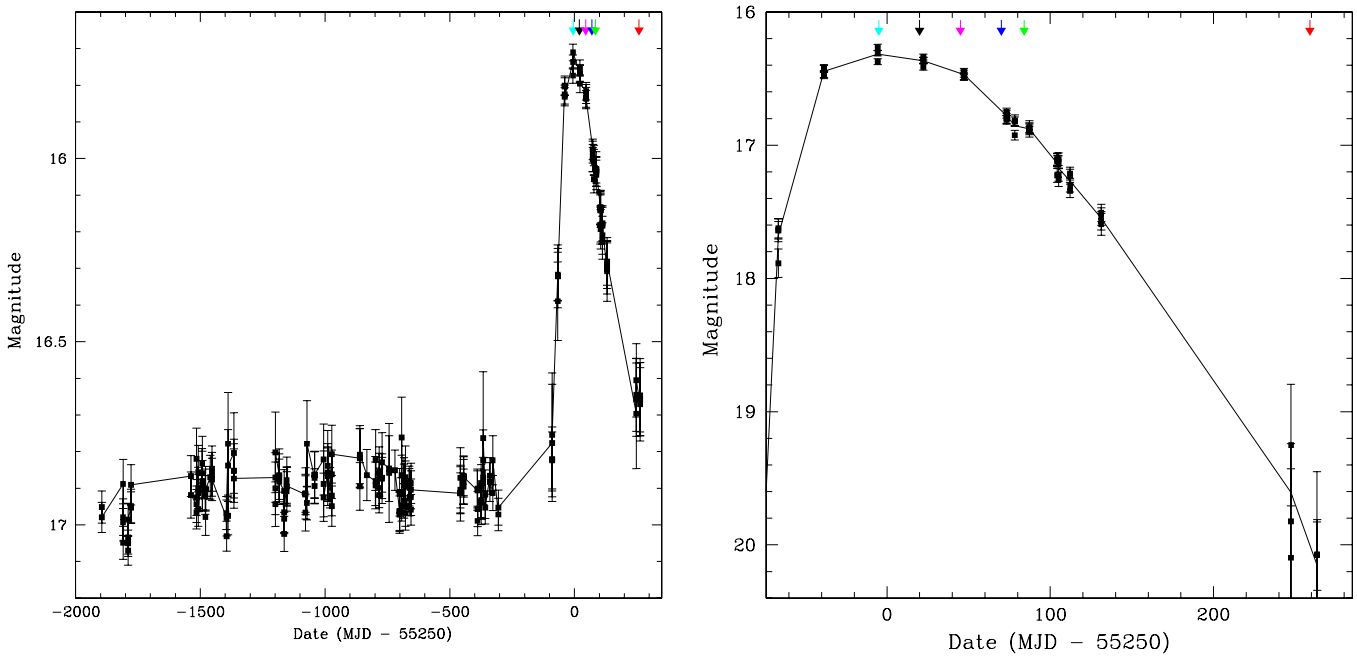

Figure 1. V_{CSS} light curves of CSS100217 taken with the 0.7 m Catalina Schmidt telescope with respect to Modified Julian Date and maximum light. Left: the full CSS light curve covering host and event. Right: the event light curve after subtracting the galaxy flux. The dates on which the IGO, P200, APO, MDM, and Keck follow-up spectra were observed are marked with arrows.

Table 3. Additional measurements in the USNO-B1.0 catalog (Monet et al. 2003) with epoch 1977.1, list the object with magnitudes $B2 = 17.6$, $R2 = 17.4$, $I = 17.2$. This suggests that the object was relative stable on a very long timescale.

Optical follow-up was taken soon after discovery with the Palomar 1.5 m telescope (P60) in gunn *g*,*r*,*i*,*z* filters. Data were also taken in Johnson *U*, *B*, *V* and Cousins *R*, *I* using the 1 m Sampurnanand telescope in Nainital, India. Data were reduced by performing point-spread function (PSF) photometry using DAOPHOT (Stetson 1987). The photometry was calibrated using Landolt's (1992) standard stars' fields PG1047+003 and PG1323-085. Ten bright isolated stars within the field of CSS100217 were used as local standards and to derive the zero points for the images of the transient. To supplement the

Table 2
CSS Photometry of CSS100217

MJD	Phase	V_{CSS}
54884.246	−365.75	16.82 ± 0.08
54884.251	−365.75	16.87 ± 0.06
54884.263	−365.74	16.76 ± 0.18
54892.171	−357.83	16.92 ± 0.07
54892.205	−357.80	16.95 ± 0.04
54911.194	−338.81	16.87 ± 0.05
54911.211	−338.79	16.88 ± 0.05
54922.299	−327.70	16.91 ± 0.05
54922.323	−327.68	16.82 ± 0.07
54945.252	−304.75	16.97 ± 0.04
54945.272	−304.73	16.95 ± 0.05
55160.445	−89.55	16.78 ± 0.16
55160.453	−89.55	16.82 ± 0.08
55160.461	−89.54	16.82 ± 0.09
55160.469	−89.53	16.75 ± 0.17
55183.410	−66.59	16.32 ± 0.09
55183.414	−66.59	16.32 ± 0.07
55183.419	−66.58	16.39 ± 0.11
55183.424	−66.58	16.32 ± 0.07
55211.379	−38.62	15.80 ± 0.03
55211.386	−38.61	15.83 ± 0.03
55211.394	−38.61	15.80 ± 0.02
55211.401	−38.60	15.83 ± 0.03
55244.284	−5.72	15.74 ± 0.02
55244.291	−5.71	15.77 ± 0.02
55244.303	−5.70	15.71 ± 0.02
55272.198	22.20	15.77 ± 0.02
55272.203	22.20	15.77 ± 0.02
55272.208	22.21	15.75 ± 0.02
55272.213	22.21	15.80 ± 0.02
55297.123	47.12	15.82 ± 0.02
55297.131	47.13	15.82 ± 0.03
55297.138	47.14	15.84 ± 0.02
55297.146	47.15	15.83 ± 0.03
55323.210	73.21	15.97 ± 0.03
55323.216	73.22	16.00 ± 0.03
55323.221	73.22	15.98 ± 0.03
55323.227	73.23	16.00 ± 0.04
55328.254	78.25	16.01 ± 0.04
55328.261	78.26	16.06 ± 0.04
55328.267	78.27	16.00 ± 0.04
55337.188	87.19	16.03 ± 0.05
55337.196	87.20	16.04 ± 0.04
55337.203	87.20	16.04 ± 0.04
55337.211	87.21	16.03 ± 0.04
55354.159	104.16	16.13 ± 0.04
55354.163	104.16	16.14 ± 0.04
55354.168	104.17	16.14 ± 0.04
55354.173	104.17	16.18 ± 0.05
55355.154	105.15	16.13 ± 0.05
55355.159	105.16	16.18 ± 0.05
55355.164	105.16	16.19 ± 0.05
55355.169	105.17	16.14 ± 0.05
55362.163	112.16	16.22 ± 0.05
55362.168	112.17	16.18 ± 0.05
55362.172	112.17	16.21 ± 0.05
55362.177	112.18	16.18 ± 0.05
55381.168	131.17	16.31 ± 0.08
55381.169	131.17	16.29 ± 0.07
55381.170	131.17	16.30 ± 0.07
55381.171	131.17	16.28 ± 0.07
55497.470	247.47	16.70 ± 0.15
55497.476	247.48	16.64 ± 0.10
55497.482	247.48	16.66 ± 0.10
55497.487	247.49	16.61 ± 0.10
55513.417	263.42	16.67 ± 0.10
55513.425	263.43	16.66 ± 0.10
55513.433	263.43	16.65 ± 0.10
55513.441	263.44	16.66 ± 0.10

Notes. The phase of the event is taken relative to the adopted maximum bright at MJD 55250. The photometry includes the flux measured for the host galaxy in the difference image template.

optical data and constrain the possibility that this was a TDE, we requested *Swift* Target of Opportunity time to observe the transient at X-ray and UV wavelengths. These observations clearly showed that the object was bright at UV wavelengths and a source was detected in the X-rays.

In Figure 2, we present the photometry of the CSS100217 during the early decline phase in six *Swift* filters $uvw1$, $uvw2$, $uvm2$, u, b, v and ground-based U, B, V, R, I. The B and b, and V and v magnitudes are in excellent agreement. However, the magnitudes vary between U and u as the Bessell filter has central wavelength 3663 Å and effective width 650 Å while the *Swift U* filter is bluer and broader (central wavelength 3465 Å, width 785 Å). Variations in the spectral energy distribution (SED) between these two filters likely causes most of the observed difference. Li et al. (2006) gives the transformation from *Swift* filters to standard Johnson filters. For b and v the difference from standard filters is of order 0.02 mag. However, for objects such as CSS100217 with $u - v < 0$ the difference noted by Li et al. (2006) is significant and the transformation to standard magnitudes is very poorly constrained. Therefore, we have not attempted to transform the *Swift* magnitudes to the standard system.

From the CSS photometry we find that the peak luminosity occurred on 2010 February 23 (MJD 55250). Hereafter we denote this date as Tp. We fit the decline rate in each photometric filter over the range of dates from $Tp + 42$ to $Tp + 112$. The observed decline of CSS100217 plus the host galaxy is close to linear and varies between bands from 0.012 mag day^{-1} in $uvm2$ to 0.0064 mag day^{-1} in I. The rapid decline at bluer wavelengths is consistent with an outburst that is cooling with time. The rate of decline is consistent with the range observed for Type IIn supernovae (Trundle et al. 2009). However, we note that the true decline rate of the transient is much greater as the photometry includes both the galaxy and transient light. In order to determine the true decline rate for CSS100217 we transformed the SDSS photometry of the host galaxy to Bessell magnitudes. As the SED of the host galaxy varies from that expected from stars, we preformed the transformation in two ways that follow Jester et al. (2005). First, we used the transformations derived for QSOs with redshift $z < 2.1$ and second for stars ($R - I_c < 1.15$ and $U - B < 0$). Using the relation for stars we obtain host galaxy flux $U = 17.55$, $B = 18.17$, $V = 17.77$, $R_c = 17.25$, and $I_c = 16.71$. With the QSO transformation we obtain $U = 17.51$, $B = 18.07$, $V = 17.77$, $R_c = 17.38$, and $I_c = 16.88$. We note that the difference in magnitudes using the two different methods is maximum for I_c (0.17 mag) and for V produces the same result. Hereafter, we adopt the transformation for stars but note that the use of the other set of equations will produce a small constant shift.

After subtracting the host flux contribution from each measurement we combined uncertainties in photometry in quadrature, with the conversion errors noted by Jester et al. (2005),

Table 3
Filtered Photometry of CSS100217 and Host Galaxy

MJD	Phase	Band1	Band2	Band3	Band4	Band5	Band6
SDSS		*u*	*g*	*r*	*i*	*z*	
52639.380	−2610.62	18.20 ± 0.01	17.84 ± 0.01	17.63 ± 0.01	17.29 ± 0.01	17.34 ± 0.01	
52639.470	−2610.53	18.17 ± 0.01	17.84 ± 0.01	17.64 ± 0.01	17.35 ± 0.01	17.36 ± 0.01	
52724.240	−2525.76	18.24 ± 0.01	17.90 ± 0.01	17.70 ± 0.01	17.38 ± 0.01	17.45 ± 0.01	
Pal. 1.5 m		*g*	*r*	*i*	*z*		
55257.248	7.25	16.43 ± 0.22	16.27 ± 0.17	16.04 ± 0.08	16.18 ± 0.12		
55257.381	7.38	...	16.48 ± 0.08	16.10 ± 0.12	16.07 ± 0.19		
55266.508	16.51	16.44 ± 0.21	16.26 ± 0.16	16.05 ± 0.19	16.30 ± 0.21		
55369.171	119.17	17.58 ± 0.19	17.31 ± 0.19	16.80 ± 0.23	16.68 ± 0.21		
55370.174	120.17	17.73 ± 0.15	17.31 ± 0.18	16.75 ± 0.21	16.68 ± 0.30		
ARIES		*U*	*B*	*V*	*R*	*I*	
55297.771	47.77	16.45 ± 0.05	16.94 ± 0.02	16.56 ± 0.01	16.38 ± 0.02	15.92 ± 0.02	
55298.799	48.80	16.52 ± 0.05	16.95 ± 0.02	16.53 ± 0.02	16.40 ± 0.04	15.87 ± 0.03	
55299.637	49.64	16.41 ± 0.06	16.93 ± 0.05	16.52 ± 0.02	16.36 ± 0.02	...	
55300.643	50.64	16.59 ± 0.06	...	...	16.40 ± 0.02	15.91 ± 0.03	
55310.656	60.66	16.55 ± 0.03	...	...	16.47 ± 0.02	15.90 ± 0.02	
55311.613	61.61	16.61 ± 0.05	17.11 ± 0.02	...	16.49 ± 0.02	± 0.02	
55312.632	62.63	16.72 ± 0.05	17.11 ± 0.04	16.67 ± 0.03	16.59 ± 0.03	15.94 ± 0.03	
55316.604	66.60	16.73 ± 0.05	17.20 ± 0.01	16.72 ± 0.01	16.58 ± 0.02	15.97 ± 0.02	
55320.610	70.61	16.68 ± 0.14	...	...	16.61 ± 0.03	16.03 ± 0.02	
55323.646	73.65	16.85 ± 0.04	17.30 ± 0.01	16.83 ± 0.02	16.71 ± 0.02	16.08 ± 0.02	
55324.601	74.60	16.89 ± 0.04	17.30 ± 0.03	16.83 ± 0.01	16.69 ± 0.03	16.09 ± 0.03	
55329.625	79.63	...	...	...	16.72 ± 0.03	...	
55334.624	84.62	16.92 ± 0.03	17.41 ± 0.03	16.97 ± 0.02	16.85 ± 0.03	16.18 ± 0.05	
55346.611	96.61	...	17.60 ± 0.02	17.10 ± 0.02	16.99 ± 0.03	± 0.03	
55349.629	99.63	17.28 ± 0.07	17.65 ± 0.05	17.14 ± 0.03	17.01 ± 0.04	16.29 ± 0.03	
55356.654	106.65	17.19 ± 0.07	17.70 ± 0.03	17.21 ± 0.02	17.14 ± 0.03	16.41 ± 0.04	
55358.620	108.62	17.25 ± 0.05	17.82 ± 0.03	17.21 ± 0.03	17.23 ± 0.05	16.49 ± 0.04	
55362.622	112.62	17.14 ± 0.04	17.77 ± 0.02	17.23 ± 0.02	...	16.49 ± 0.04	
55364.619	114.62	...	17.80 ± 0.06	17.19 ± 0.06	...	16.49 ± 0.04	
55495.983	245.98	...	19.49 ± 0.20	18.61 ± 0.08	19.15 ± 0.20	17.64 ± 0.10	
55499.932	249.93	18.97 ± 0.20	19.18 ± 0.09	18.74 ± 0.09	19.43 ± 0.25	17.77 ± 0.09	
55509.979	259.98	19.28 ± 0.24	19.41 ± 0.09	18.58 ± 0.06	19.20 ± 0.19	17.99 ± 0.13	
55527.971	277.97	18.84 ± 0.19	...	18.97 ± 0.10	20.58 ± 0.77	...	
55533.979	283.98	19.10 ± 0.28	19.97 ± 0.18	19.10 ± 0.10	20.68 ± 0.86	17.96 ± 0.29	
55562.971	312.97	19.41 ± 0.30	21.11 ± 0.49	19.41 ± 0.13	...	18.24 ± 0.30	
Swift		*UVW1*	*UVM2*	*UVW2*	*U*	*B*	*V*
55292.580	42.58	16.10 ± 0.03	16.09 ± 0.02	16.27 ± 0.02	15.76 ± 0.03	16.55 ± 0.03	16.18 ± 0.04
55311.620	61.62	16.19 ± 0.10	16.44 ± 0.07	16.43 ± 0.03	15.90 ± 0.03	16.80 ± 0.03	16.32 ± 0.04
55325.940	75.94	16.39 ± 0.03	16.46 ± 0.03	16.64 ± 0.03	16.07 ± 0.03	16.84 ± 0.03	16.35 ± 0.04
55339.120	89.12	16.78 ± 0.06	16.66 ± 0.08	16.71 ± 0.02	16.17 ± 0.06	16.98 ± 0.03	16.56 ± 0.04
Near-IR		*J*	*H*	K_s			
55312.176	62.18	15.06 ± 0.11	14.19 ± 0.13	13.54 ± 0.09			
55313.311	63.31	15.23 ± 0.12	14.38 ± 0.14	13.44 ± 0.12			
55333.230	83.23	15.03 ± 0.10	14.28 ± 0.12	13.17 ± 0.11			
55336.209	86.21	15.22 ± 0.11	14.18 ± 0.13	13.03 ± 0.10			
55338.175	88.18	14.99 ± 0.11	14.38 ± 0.14	13.69 ± 0.09			
55340.162	90.16	15.59 ± 0.13	14.46 ± 0.12	13.74 ± 0.10			
55342.155	92.16	15.41 ± 0.11	14.32 ± 0.12	13.51 ± 0.10			
55361.191	111.19	15.15 ± 0.11	14.09 ± 0.12	13.17 ± 0.09			
55369.147	119.15	15.52 ± 0.11	14.33 ± 0.12	13.72 ± 0.09			

Notes. The phase of the event is taken relative to the adopted maximum bright at MJD 55250. SDS photometry is that of the host galaxy. *Swift* photometry measurements include the flux from the host galaxy. All other photometry have the host galaxy flux subtracted.

then fit each with a simple linear decline over the time between $Tp + 42$ and $Tp + 112$. The following declines rates were found: $\Delta U = 0.0121(0.0017)$, $\Delta B = 0.0134(0.0018)$, $\Delta V = 0.0112(0.0026)$, $\Delta R = 0.0132(0.0021)$, $\Delta I = 0.00985(0.0019)$. The slope derived from the CSS light curve during this period was $\Delta V_{\rm CSS} = 0.0117(0.0022)$, and thus is very close to that observed in the filtered V photometry. For the Palomar 1.5 m photometry in the gunn filter system matches that of SDSS, therefore, we subtract the SDSS host magnitudes. The host-subtracted-filtered optical photometry from Palomar 1.5 m and ARIES 1 m is presented in Table 3, as is the *Swift* photometry for this event.

Based on our filtered photometry, the CSS transformed V magnitudes ($V_{\rm CSS}$) lie very close to R magnitudes. The decline rate is also very similar. The $V_{\rm CSS}$ values are slightly brighter than filtered V magnitudes ($\Delta V < 0.2$ mag). The departure of

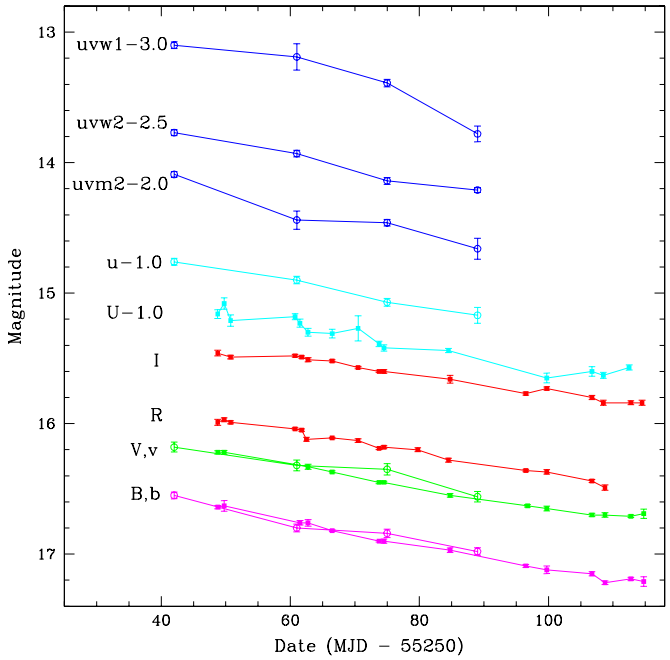

Figure 2. Multicolor evolution of CSS100217 near peak from the *Swift* space telescope and ARIES 1 m. *Swift* UVOT observations are in *uvw1*, *uvw2*, *uvm2*, *u*, *v*, and *b* bands. ARIES observations are in Johnson *U*, *B*, *V* and Cousins *R* and *I* bands.

(A color version of this figure is available in the online journal.)

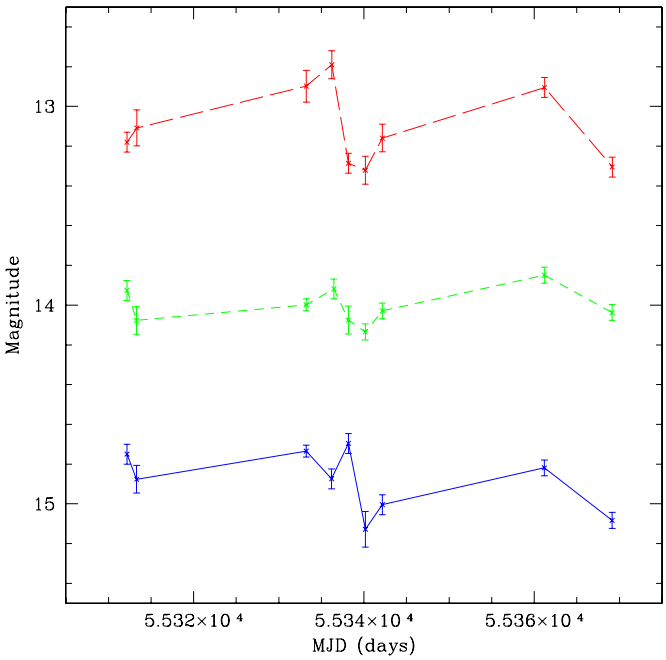

Figure 3. Near-IR light curves of CSS100217 in *J*, *H*, and K_s bands. The short-dashed line presents the observed K_s-band values, the long-dashed line connects *H*-band measurements, and the solid line *J*-band magnitudes.

(A color version of this figure is available in the online journal.)

CSS photometry from Bessell *V* is due to the non-stellar SED of the transient source combined with the galaxy. In particular, the strong H_α emission lies within the CSS transmission sensitivity as well as the overlap between *R* and *I* filter response (well beyond *V* filter response).

The foreground Galactic extinction for this event is $A_V = 0.046$, based on Schlegel et al. (1998) reddening maps. We do not see evidence for host galaxy extinction in the spectra of event, suggesting this is a small effect. Thus, we only correct for foreground extinction. Applying the *V*-band reddening correction and a *K*-correction of 0.15 mag, to account for the effective rest-frame bandwidth, we find that the peak luminosity was $M_{V_{\rm CSS}} = -23.0$. We adopt $H_0 = 72$ km s^{-1} mpc^{-1}, $\Omega_\Lambda = 0.73$, and $\Omega_m = 0.27$ with the host galaxy's redshift of $z = 0.147$. To derive K-correction in filtered photometry near peak we first subtracted the SDSS spectrum from the IUCAA Girawali Observatory (IGO) follow-up spectrum observed near peak. Using the Palomar spectrum that was taken near maximum light ($Tp + 20$ days), we derive the *K*-corrections in the *V* and *R* filters of −0.01 and 0.04, respectively. As the filter transmission range of our other filtered observations goes beyond that of this spectrum (3950–9050 Å), K-corrections are not derived for other filters.

The extinction and *K*-corrected peak magnitudes measured at $Tp + 40$ are $M_V = -22.7 \pm 0.3$ and $M_R = -22.8 \pm 0.3$. Here, we have combined estimates for uncertainties in the true color variation near peak (0.1), the photometric zero points (0.15), the *K*-corrections (0.1), and the color transformations from SDSS filters (0.17). For the Palomar 1.5 m gunn photometry taken at $Tp + 7$, we use the IGO spectrum taken at $Tp - 5$ and find a *K*-correction of $K_r = -0.16$ and thus $M_r = -22.8 \pm (0.3)$. Here, there is no need to transform the filter system as the observations are not long after maximum. However, the photometric uncertainties are larger. For the other gunn measurements taken at this time we find $M_g = -22.8$, $M_r = -23.0$, $M_i = -23.2$, and $M_z = -23.1$, without *K*-correction. Similarly, for ARIES photometry, taken at Tp+40, we find $M_U = -22.9$, $M_B = -22.3$, and $M_I = -23.3$, without *K*-correction.

The peak brightness in *V* band is similar to that observed for the Type IIn supernovae SN 2008fz (Drake et al. 2010a, $M_V = -22.3$) and Type IIL supernova SN 2008es ($M_V = -22.2$, Gezari et al. 2009b; $M_V = -22.3$, Miller et al. 2009). Another luminous Type IIn, SDWFS-MT-1 (aka SN 2007va) was detected in *Spitzer* data and was observed with $M_{[4.5]} \sim -24.2$ in 4.5 μm *Spitzer*/IRAC band (Kozlowski et al. 2010).

Near-IR *J*, *H*, and K_s observations were carried out with CANICA, a NIR camera equipped with a 1024 × 1024 pixel Hawaii array, at the 2.1 m telescope of the Guillermo Haro Observatory located in Cananea, Sonora, Mexico. Data were reduced using standard procedures. As some observations were carried out on partially cloudy nights, differential photometry for the object and field stars was carried out. For the latter, we adopted the photometric values listed in the 2MASS All-Sky Catalog of Point Sources (Skrutskie et al. 2006). In Figure 3, we present the near-IR measurements and in Table 3 we include the host-subtracted near-IR photometry. The peak-observed apparent brightness of CSS100217 in near-IR, after subtracting the host brightness using 2MASS magnitudes, is $J \sim 15.0$, $H \sim 14.1$, and $K_s \sim 13.0$. The corresponding absolute magnitudes are thus $M_J = -24.2$, $M_H = -25.1$, and $M_{K_s} = -26.2$ (again without *K*-correction). However, we note that there may be significant uncertainty in the near-IR brightness of the transient. Once the event has fully faded, it will be possible to determine the host contribution more accurately and thus the event's peak brightness in each filter. Unlike the optical data there is little evidence for a decline in luminosity. This effect may be attributed to the cooling of expanding material. The object is

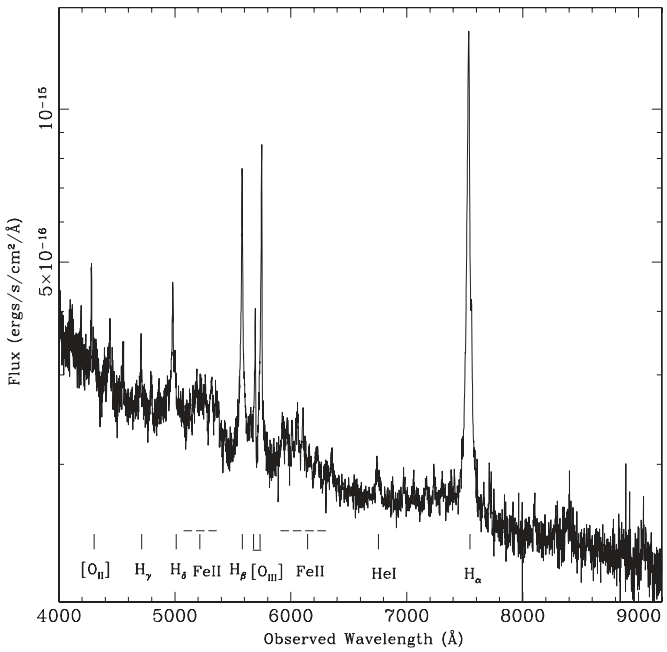

Figure 4. Archival SDSS DR7 spectrum of the host galaxy to CSS100217 (SDSS J102912.58+404219.7).

brighter than 2MASS in the near-IR follow-up observations by $\Delta J \sim 1.6$, $\Delta H \sim 1.45$, and $\Delta K \sim 1.35$ mag. Strong near-IR excess has been observed in many Type IIn supernovae and has been interpreted as thermal emission from dust in a pre-existing circumstellar nebula (Gerardy et al. 2002). If CSS100217 is a Type IIn supernova, near-IR emission is expected to increase at first and then gradually decline over the coming years.

The host galaxy, SDSS J102912.58+404219.7, was serendipitously observed by the *GALEX* All-Sky Imaging Survey on 2004 January 24 with FUV = 19.52 ± 0.17 and NUV = 18.97 ± 0.08 mag, and by the Medium Imaging Survey on 2010 January 29 with NUV = 17.078 ± 0.009 mag (Gezari et al. 2010). A request for follow-up *GALEX* observations was made after these archival observations revealed that the event had brightened in the NUV filter by 1.9 mag, ∼1.5 months before the optical maximum. We obtained NUV imaging on 2010 April 17 and 29, which measured NUV = 17.756 ± 0.012 and 17.881 ± 0.015 mag, respectively, indicating that the event had faded by 0.8 mag in the NUV 3 months later. The *GALEX* magnitudes are in the AB system and have been corrected for the energy lost in a 6″ radius aperture and for Galactic extinction.

3.2. Optical Spectra

3.2.1. The Nature of the Host Galaxy

When CSS100217 was discovered it was immediately recognized as an unusual object. Analysis of the SDSS DR7 (Abazajian et al. 2009) spectrum of the host galaxy (SDSS J102912.58+404219.7) suggested that the object was a Seyfert. However, the rate and degree of variability had never been encountered during the prior years of the CRTS transient survey, nor in previous transient searches carried out by the PQ survey (Djorgovski et al. 2008). In Figure 4, we present the spectrum obtained by the SDSS in 2002 December. The spectrum is reminiscent of an AGN with clear strong Balmer, [O II] and [O III] emission lines. AGNs viewed away from the line of sight of the jet exhibit smooth light curves that increase in variability on long timescales (Webb & Malkan 2000). In contrast optical variability of many magnitudes can be seen in blazars (Bauer et al. 2009) which have broad lines and are associated with strong radio sources and have smooth featureless continua during their outbursts. In this case the emission lines observed from the galaxy were relatively narrow and no radio detection has been made in past radio surveys by FIRST (1.4 GHz, Becker et al. 1995), WENSS (326 mHz, Rengelink et al. 1997), and NVSS (1.4 GHz, Condon et al. 1998) at the level of 1 mJy beam^{-1}.

The emission line features observed in the SDSS spectrum are very clearly asymmetric. In addition, the Balmer lines appear to have a broad component. We decomposed the SDSS spectrum to determine the nature of the SDSS source. For H_β we see three clear significant components with narrow, medium, and broad velocity widths. There were clearly systematic offsets between the broad-, medium-, and narrow-line components. For [O III] we found just narrow and medium width components that were consistent with the H_β emission features. For the H_α region the line fitting process is more complex because of the presence of blended N II emission lines. First, we fit the line complex with individual [N II] 6548 Å and 6583 Å lines of fixed 1/3 flux ratio plus H_α emission lines considering just a narrow and broad component. The fit result was quite poor as the H_α has broad wings and an asymmetric peak. The [N II] lines were also poorly modeled. We then decided to add a medium width component to the [N II] and H_α emission to match that expected given the H_β and [O III] lines. Next, we simultaneously fit the H_β and H_α with three velocity components, and the [O III] and [N II] with two components. In Figure 5, we present the fits to these lines. In Table 4, we present the flux, velocity, and central wavelength values obtained for the emission lines including both models for the H_α region.

In Figure 6, we present the standard Baldwin et al. (1981, hereafter BPT) emission-line diagnostic diagrams used to separate AGNs from starburst galaxies. We include points using the fit values given in Table 4, along with the emission line galaxies presented in the MPA/JHU version of the SDSS DR4 catalog (Kauffmann et al. 2003; Adelman-McCarthy et al. 2006). Here we have selected galaxies largely following Kewley et al. (2006). That is, only galaxies having emission lines with S/N > 3 in each line species and S/N > 20 in the spectrum were selected. Galaxies were selected in the redshift range $0.04 < z < 0.17$. The sample consists of ∼135,000 objects. For comparison, we have also plotted the NLS1 from Zhou et al. (2006) that contain flux measurements for H_α, H_β, and [N II].

We have not included the standard [O III]/H_β versus S II/H_α diagnostic diagram as we found that the location of redshifted [S II] corresponds to the location of a strong sky emission line in the raw SDSS spectrum. We found that the ratio of S II/H_α is much lower than observed in other SDSS emission-line galaxies. This is likely due to poor subtraction of the strong sky line. In Figure 6, we show the theoretical demarcation lines separating emission-line galaxies as determined by Kewley et al. (2001) as well as the empirical demarcation lines of Kauffmann et al. (2003) and Stasinska et al. (2006). The galaxy appears in the starburst region of the [O III]/H_β versus [N II]/H_α but in either starburst or AGN region for [O III]/H_β versus [O I]/H_α. This suggests that the object may be a combination object having both starburst and AGN features.

In Figure 7, we present the location of the host in relation to the new emission-line diagnostic diagram of Kewley et al. (2006). Here the SDSS source lies within the Seyfert region. However, of the 921 NLS1 with H_α values we selected from Zhou et al.

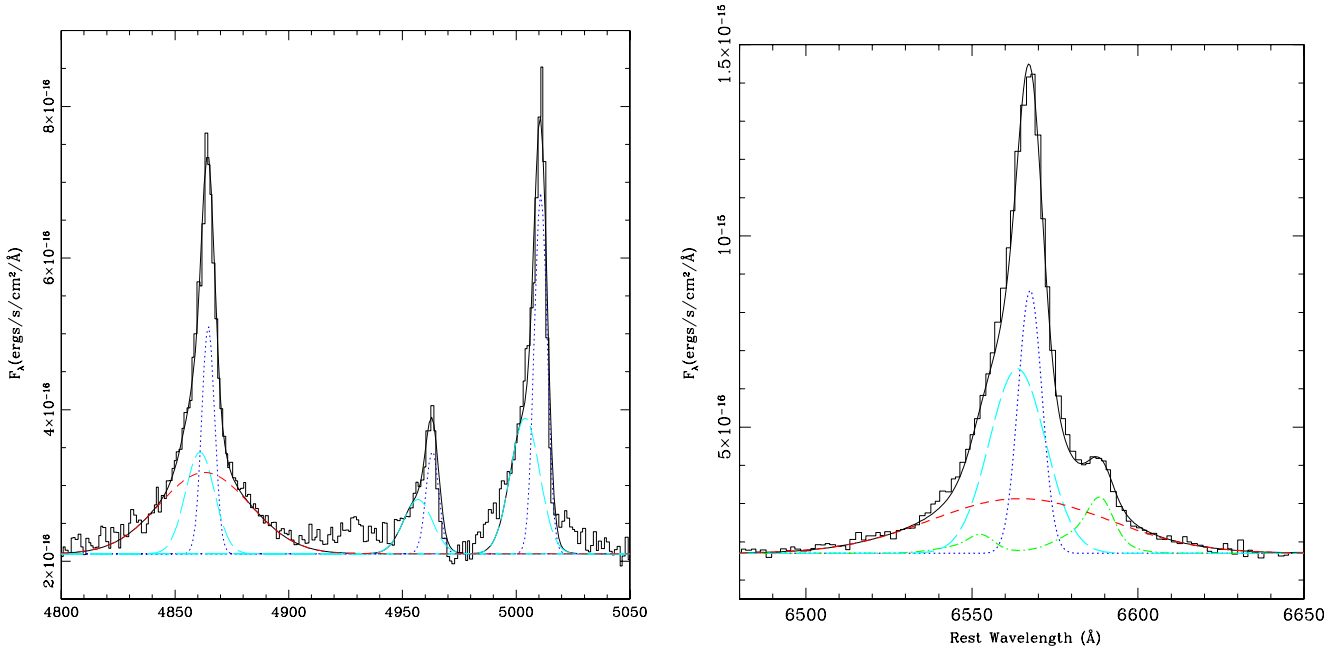

Figure 5. Host galaxy emission-line fits. Dotted line: narrow components of H_β, H_α, and [O III]. Long-dashed line: intermediate velocity components. Short-dashed line: broad H_α and H_β components. Solid line: overall fit.

(A color version of this figure is available in the online journal.)

(2006), only 32 lie in the starburst region of Kauffmann et al. (2003) in [O III]/H_β versus [N II]/H_α and 16 lie in this region for the stricter starburst–AGN separation line of Stasinska et al. (2006). Clearly the host is not a typical NLS1. Indeed, the location of the object to the left of the AGN–starburst composite objects suggests that the amount of star formation is significant. Three similar objects were investigated by Mao et al. (2009). In that case one of the three objects was within the starburst region on the diagrams, whereas two were within the composite region in the [O III]/H_β versus [N II]/H_α diagram. Mao et al. explain the reason for the locations of these objects as AGNs buried in H II regions where they are transitioning from a starburst-dominated phase to an AGN-dominated phase.

The presence of broad Balmer components within the SDSS spectrum is clear and strongly suggests the presence of an AGN. Core-collapse Type II supernovae and stellar winds from massive stars can also produce such broad lines. Izotov et al. (2007) discussed the possibility of multiple supernova events and massive star-forming regions and noted that broad lines can arise from these sources. The SDSS spectrum was taken on 2003 December 29, while our first CSS observations of the object were in 2004 December. If a supernova had occurred in the galaxy in 2003, it would have faded by the time we first observed it. However, the likelihood of such an event is not large. Mao et al. (2009) also discussed this possibility for their three objects.

The NLS1 nature of the host galaxy is further supported by the [Ne V] λ3426 emission line. NLS1 exhibit strong Fe II emission features as seen in the SDSS spectrum. However, Type IIn supernovae also exhibit strong Fe II lines in late spectra. The width of the broad H_α and H_β emission lines is ∼2900 km s^{-1}. This is significantly broader than the 2000 km s^{-1} limit expected for NLS1. The observed line width is consistent with that observed in the late time spectra of Type IIn. Nevertheless, the combination of the line diagnostics and spectral features with the low likelihood of observing two Type IIn supernovae in the same galaxies within a period of a few years suggests that the SDSS source is an NLS1 and also has significant ongoing star formation.

Table 4
SDSS Spectrum Emission Lines

Feature	Flux (1E-17 erg cm^{-2} s^{-1})	λ (Å)
$H_{\beta b}$	750	4863.0
$H_{\beta m}$	300	4861.5
$H_{\beta n}$	297	4864.6
$[O\,III]_{4959m}$	160	4956.8
$[O\,III]_{4959n}$	134	4963.2
$[O\,III]_{5007m}$	470	5003.9
$[O\,III]_{5007n}$	400	5010.8
[O I]	81	6306.6
[S II]	75	6722.1
[S II]	...	6736.2
$H_{\alpha b}$	1400	6564.4
$H_{\alpha m}$	1490	6563.7
$H_{\alpha n}$	900	6567.5
$[N\,II]_m$	250	6548.5
$[N\,II]_n$	163	6552.8

Notes. Subscripts *b*, *m*, and *n* denote the broad, medium, and narrow components, respectively. The FWHM fit values for these components are 2899, 911, and 376 km s^{-1}, respectively. The velocity measurements are corrected for instrumental dispersion.

3.2.2. *Follow-up Spectroscopy*

Following the discovery of CSS100217 we immediately scheduled spectroscopic observations with the IGO 2 m telescope. These observations were taken on February 18 and showed an outburst spectrum similar to the archival SDSS

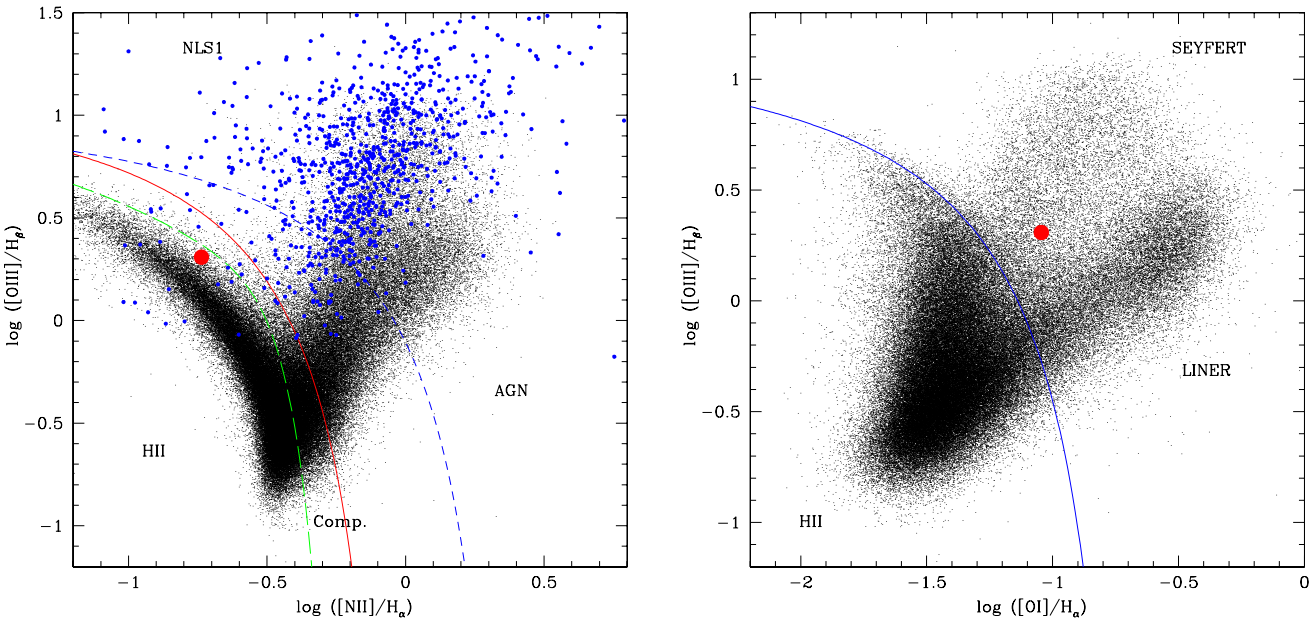

Figure 6. Comparison of the host galaxy abundances relative to the SDSS emission-line galaxies. The large solid dot shows the location of CSS100217 based on values from Table 4. Left: the large dots give the locations of known NLS1 galaxies from Zhou et al. (2006). The dashed line shows the Kewley et al. (2001) theoretical division between starburst and AGN galaxies. The solid line shows the division found by Kauffmann et al. (2003) and the long-dashed line shows the division determined by Stasinska et al. (2006). Right: the dashed line shows the Kewley et al. (2001) theoretical division between starburst and AGN galaxies.

(A color version of this figure is available in the online journal.)

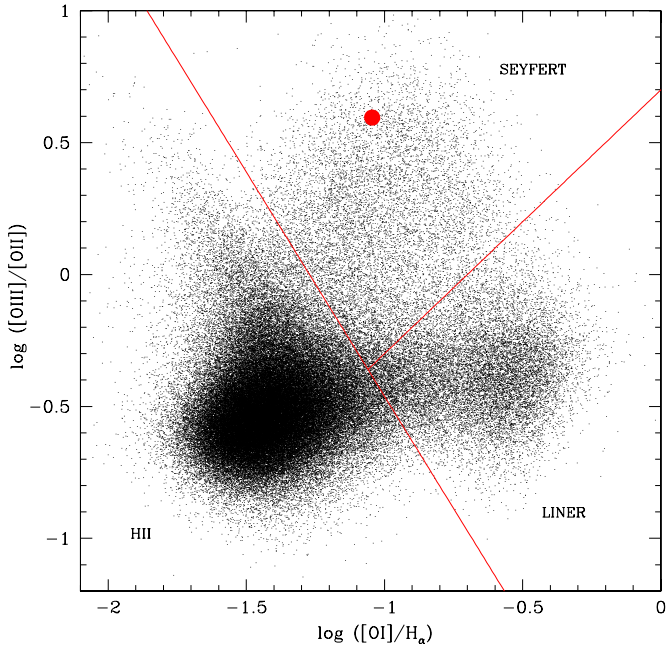

Figure 7. Comparison of the host galaxy abundances relative to the SDSS emission-line galaxies. The large solid dot shows the location of CSS100217 based on values from Table 4. The lines show the Kewley et al. (2006) division between Seyfert, liner, and starburst galaxies.

(A color version of this figure is available in the online journal.)

spectrum. The spectrum clearly exhibited a much bluer continuum and Balmer lines that were stronger by a factor of ∼5, consistent with a Type II supernova. Upon subtraction of the SDSS spectrum from IGO data there was no evidence for a change in [O II] and [O III] and Fe emission lines. However, the spectrum did not appear to exhibit a significant new broad H_α component relative to the SDSS spectrum as expected for IIn supernovae. Interpretation of the event was complicated by its location near what was suspected to be an AGN. In order to confirm the initial result we scheduled additional IGO spectra and took a Palomar 5 m spectrum on March 15. The Palomar spectrum was found to be very similar to the initial IGO one but exhibited a slightly shallower continuum slope. Subsequently we obtained spectroscopic follow-up with IGO, Apache Point Observatory (APO), MDM, and Keck. These spectra do show signs of a new broad component not present in the SDSS spectrum. In Figure 8, we present follow-up spectra of CSS100217 spanning the period from 2010 February 18 to May 18. In Figure 9, we present these same spectra after subtracting the archival SDSS spectrum of the host galaxy.

A test for whether CSS100217 may be due to AGN activity can be derived from changes in the emission-line characteristics. Narrow emission lines are potentially more useful for this test than broad emission lines because they are powered by the average ionizing flux over decades, rather than over days for broad emission lines (Halpern et al. 2003).

To examine the spectroscopic changes in more detail, for each spectrum, we subtracted the fits to the SDSS emission lines from the H_α and H_β line profiles and fit the residual emission lines. In Table 5, we present the fluxes and line widths for the residuals. The removal of the constant [O III] lines from the host galaxy was found to be relatively complete for IGO, Palomar, MDM, and Keck spectra. This suggests that the flux calibration is good. We believe that the errors in the remaining emission-line fluxes are ∼20% due to calibration uncertainties. However, the measurements may be higher for Balmer components since the CSS and SDSS photometry suggests that the AGN was in a lower state when it was spectroscopically observed by SDSS. The spectra with uncertain flux calibration were not analyzed in this work.

In Figure 10, we display the fit to the residual H_α flux from our November 9 Palomar spectrum when the event had faded significantly. Clearly, unlike the SDSS spectrum, the emission exhibits a strong broad component. However, the narrow component is of the same width as the SDSS spectrum

Table 5
CSS100217 Emission-line Properties

Observation	MJD	Phase	$H_{\beta b}$	$H_{\beta m}$	$H_{\beta n}$	$H_{\alpha b}$	$H_{\alpha m}$	$H_{\alpha n}$
FWHM (km s^{-1})								
IGO_{Feb}	55245	−5	2106	...	465	2814	1126	323
$P200_{Mar}$	55270	20	2614	...	610	3190	1126	323
MDM	55320	70	3630	2106	435	...	1219	320
Keck	55334	84	4357	1423	407	4879	1219	347
$P200_{Nov}$	55509	164	4304	1772	405	3843	1406	328
Flux (10^{-17} erg cm^{-2} s^{-1})								
IGO_{Feb}	55245	−5	2105	...	1195	4136	1126	1259
$P200_{Mar}$	55270	20	2210	...	1334	4136	1126	1888
MDM	55320	75	2280	1228	1501	...	1219	2727
Keck	55334	84	2315	842	438	7031	1219	2937
$P200_{Nov}$	55509	164	2877	2105	702	8686	1406	1888

Notes. Balmer emission-line velocity widths in km s^{-1}. Phase is taken relative to the maximum light at MJD 55250. Subscripts *b*, *m*, and *n* denote the broad, medium, and narrow components, respectively. Velocity measurements are not corrected for instrumental dispersion. Palomar spectra taken in 2010 March and 2010 November are noted as $P200_{Mar}$ and $P200_{Nov}$, respectively, and the IGO spectrum from 2010 February is noted as IGO_{Feb}.

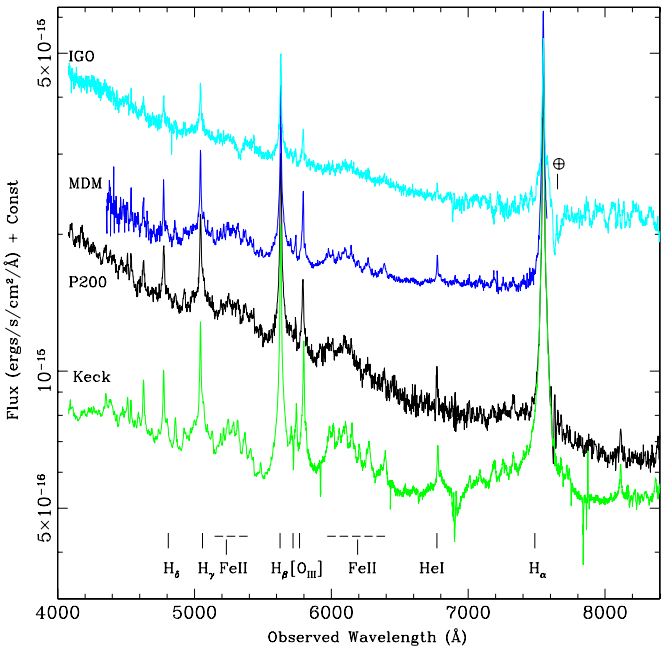

Figure 8. Spectra of CSS100217 at $\tau = 1$ (IGO), $\tau = 26$ (P200), $\tau = 76$ (MDM), and $\tau = 90$ days (Keck) after discovery. Maximum light occurred at $\tau \sim 6$. Data shown were obtained with the IGO 2 m, Palomar 5 m + DBSP, MDM 2.4 m, and Keck 10 m + LRIS.

(A color version of this figure is available in the online journal.)

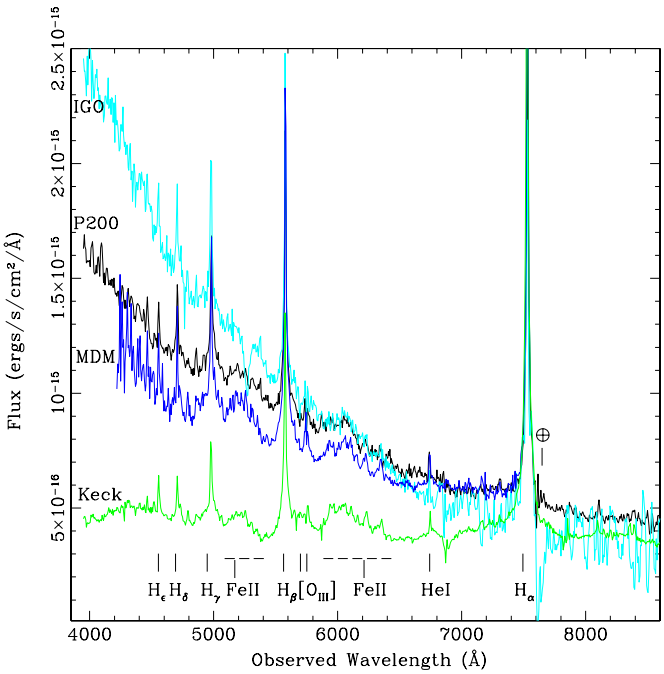

Figure 9. Host-galaxy-subtracted follow-up spectra of CSS100217, taken between 2010 February 18 and May 18, as per Figure 8.

(A color version of this figure is available in the online journal.)

and the medium component is significantly narrower than that seen in the SDSS spectrum. The flux ratio of $H_{\alpha b}$ to $H_{\alpha n}$ in the late Palomar data is 4.6 after subtracting the SDSS contribution. This is very different from that found in the SDSS spectrum (1.4). The total H_α flux is observed to increase with time, while the continuum and optical luminosity decreases. Both H_β and H_α exhibit a new broad component with width $\sim$4000 km s^{-1} that increases in velocity with time. However, unlike H_α, H_β shows little change in total flux with time.

As noted above, the light curve (Figure 1) shows an increased brightness at the end of 2004. This variation is interpreted as largely due to AGN activity and suggests that the source was fainter at the time that the SDSS spectrum was observed. Therefore, some of the flux observed in our SDSS-subtracted spectra is likely due to the host flux being incompletely subtracted. Slight differences between the SDSS and follow-up spectra may also arise from the 3″ diameter fiber used by SDSS. This fiber is large enough to contain the bulk of the light from the host, whereas long-slit spectra with widths $\sim$1″ were used for transient follow-up observations. However, our *Hubble Space Telescope* (*HST*) images suggest that almost all of the flux from the host and CSS100217 lies within the central 1″. No second contributing source is seen within 3″.

In addition to optical spectra we obtained *GALEX* NUV grism observations on 2010 April 17 and 2010 April 29. We detected emission near rest wavelength 1910 Å which likely corresponds to [C III] (λ1909). This emission is clearly detected and has an intrinsic width of 3900 ± 500 km s^{-1}. Such emission is seen in NLS1 galaxies (Leighly & Moore 2004) but is also associated

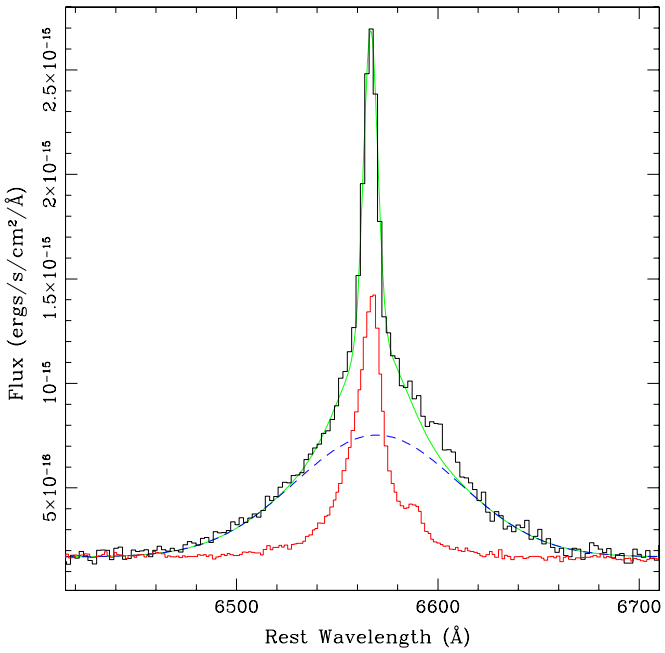

Figure 10. Fit to outburst H_α emission observed with Palomar 5 m on 2010 November 9. The red line shows the SDSS profile and the black line the Palomar data after subtracting the SDSS fit. The green line shows the three-component fit. The dashed blue line shows the broad H_α component.

(A color version of this figure is available in the online journal.)

with circumstellar emission and ejecta in Type IIn supernovae (Fransson et al. 2005; Cooke et al. 2010). We did not detect any variability over the 12 days between the two epochs.

3.3. Energetics of CSS100217

The extreme luminosity of CSS100217 is a clear sign of the energy powering this event. In order to determine the amount of optical energy expended we follow the calculations of the energetic Type IIn supernova SN 2003ma given by Rest et al. (2011). The bolometric luminosity in band X can be defined as

$$L_{\mathrm{bol},X} = b_X L_{\odot,X} 10^{(M_{\odot,X}-(M_X)/2.5}, \quad (1)$$

where the solar constants for filters $X = (V, R)$ are $M_{\odot,X} = (4.83, 4.42)$ and $L_{\odot,X} = (4.64, 6.94) \times 10^{32}$ erg s^{-1}, respectively (Binney & Merrifield 1998). The absolute magnitude of the event in filter X, M_X, is determined from the corrected photometry and b_X is the bolometric correction. As noted in the previous section, the event exhibits significant spectroscopic evolution during the event. Thus, the bolometric correction and the K-correction applied to determine M_X vary with time. In order to account for this variability, we use the IGO, P200, APO, MDM, and Keck calibrated spectra from Table 1. The spectra are spread out over intervals of roughly 20 days, accounting for 90 days when the event was emitting the most energy near peak luminosity. K-corrections are determined for V and R filters by integrating the event spectra combined with the known filter transmissions. As the redshift is relatively small, the spectra cover both the rest and observed V-passband wavelength range and we calculate in-band (V_{obs} to V_{rest}) K-corrections, rather than cross-band corrections (e.g., R_{obs} to V_{rest}).

The early spectra of CSS100217 show the clear presence of a hot continuum component that is a good fit to a blackbody of temperature 1.6×10^4 K in the rest frame. The *GALEX* UV photometry from 2010 January 29 also supports this result.

Table 6
Correction Parameters

Spectrum	Phase	BB_T	K_V	K_R	b_V	b_R
IGO	−5	16.2 ± 1.8	−0.13	−0.11	23.6	25.1
P200	20	13.5 ± 0.8	−0.01	0.04	15.2	14.2
APO	45	12.5 ± 0.8	−0.08	0.12	14.8	12.1
MDM	70	11.5 ± 1.2	0.02	0.08	12.2	10.0
Keck	84	7.8 ± 2.0	0.21	0.36	7.4	4.1

Notes. Column 1 gives the source of the spectrum used to determine corrections. Column 2 gives the time of the spectrum relative to the adopted maximum light at MJD 55250. Column 3 gives the blackbody fit temperature in kK. Columns 4 and 5 give the K-correction in V and R bands, respectively. Columns 6 and 7 give the bolometric correction in V and R bands, respectively.

At this temperature much of the energy is emitted at rest-frame wavelengths shorter than the observed in optical spectra ($\lambda < 3440$ Å). At later times the blackbody emission component has cooled to $\sim 8 \times 10^3$ K and far less flux is emitted at blue wavelengths. Therefore, in order to determine the bolometric correction, we must account for this emission and its evolution. We fit the continuum component of the host-galaxy-subtracted spectra taken between $Tp - 5$ and $Tp + 84$ with a blackbody. The linear fit to the temperature of the blackbody component in these spectra gives a cooling rate of 73.0 ± 0.5 K day^{-1}. At the time the second Palomar spectrum was taken, $Tp + 164$, the amount of additional continuum flux from CSS100217 is too small to provide an accurate blackbody fit, so we adopt the Keck values.

To approximate the full SED for the event, we combine our observed spectra with the blackbody for wavelengths $\lambda <$ 3440 Å. We then integrate the complete model fluxes and those expected with response expected within the V and R passbands. Since we do not know the exact response of the unfiltered CSS data, we cannot determine accurate K-corrections for V_{CSS} photometry. In Table 6, we present the bolometric corrections and K-corrections determined from the SED models. At early times the bolometric correction is large because of the hot component and at later is much closer to values from a solar SED.

In order to determine the bolometric luminosity of the event we correct the filtered V and R photometry (from ARIES, Table 3) for extinction and K-corrections from the spectra taken nearest the observing time. In all cases these corrections are small. To determine the total bolometric luminosity we integrated the values of $L_{\mathrm{bol},V}$ and $L_{\mathrm{bol},R}$ during the period when the filtered and unfiltered photometry completely overlap ($Tp+40$ to $Tp+230$). The resulting values are $E_{\mathrm{bol},Vp} = 3.6 \times 10^{51}$ erg and $E_{\mathrm{bol},Rp} = 2.9 \times 10^{51}$ erg. The subscript p denotes that this is only for the overlapping period. The corresponding values without bolometric correction are $E_{Vp} = 3.9 \times 10^{50}$ and $E_{Rp} = 4.4 \times 10^{50}$ erg, respectively. The corresponding average bolometric corrections over this period are $\bar{b}_V = 9.3$ and $\bar{b}_R = 6.6$.

In order to estimate energy values for the entire event we first assumed the V-band corrections for CSS photometry covering the entire V_{CSS} light curve. The total integrated bolometric luminosity is $E_{\mathrm{bol},V_{\mathrm{CSS}}} = 1.3 \times 10^{52}$ erg and $E_{V_{\mathrm{CSS}}} = 8.5 \times 10^{50}$ erg without bolometric correction. The bolometric correction averaged over the complete CSS light curve is $\bar{b}_{V_{\mathrm{CSS}}} \sim 15$. This factor is large due to much of the energy being expended at short wavelengths near peak when the event had a temperature $\sim 1.6 \times 10^4$ K. Nevertheless, as these data

lack an accurate K-correction we favor the values determined from the filtered ARIES photometry.

Next, we determined the integrated luminosity for the CSS data taken during the period when both filtered and unfiltered observations were made (Tp + 40 to Tp + 230) and found $E_{\mathrm{bol},V_{\mathrm{CSS}}p} = 3.8 \times 10^{51}$ erg. This measurement is very close to the value from filtered V photometry ($E_{\mathrm{bol},Vp} = 3.6 \times 10^{51}$ erg). The ratio of energy from the full CSS light curve ($E_{\mathrm{bol},V_{\mathrm{CSS}}}$) to $E_{\mathrm{bol},V_{\mathrm{CSS}}p}$ is ∼3.5. This provides an estimate of the fraction of energy expended during the entire event relative to the period when filtered observations were taken.

We thus estimate the total bolometric luminosities for the filtered photometry by multiplying by this factor (∼3.5). We find $E_{\mathrm{bol},V} \sim 1.3 \times 10^{52}$ and $E_{\mathrm{bol},R} \sim 1.0 \times 10^{52}$ erg. Since we have applied the correction based on the CSS light curve data, the average bolometric correction over the entire event is approximately the same as for the CSS data (∼15). The correction factor is larger than has been found for other supernova of similar temperature. The reason for this likely due to the difference in the SED from other types of supernovae. The uncertainty in these values is expected to be of order 25% due to photometric errors, sparse sampling of the CSS light curve near peak, variation of the spectra with time, uncertainty in spectroscopic flux calibration, and variations in the flux ratio for filtered and unfiltered response. As these measurements are based on 287 rest-frame days it is likely that a slightly higher value would be found for the full light curve.

In comparison to CSS100217, a number of very energetic Type IIn supernovae have recently been discovered. Rest et al. (2011) found the past Type IIn supernovae, SN 2003ma, expended 4×10^{51} erg (with a bolometric correction of ∼3.4) and Drake et al. (2010a) obtained a value of $>1.4 \times 10^{51}$ erg (without bolometric correction) for the Type IIn supernova SN 2008fz. Similarly, Kozlowski et al. (2010) found that the Type IIn supernova, SDWFS-MT-1, expended $>10^{51}$ erg in the 4.5 μm *Spitzer*/IRAC band. Smith et al. (2010a) found that the Type IIn supernova SN 2006gy had an integrated bolometric luminosity of at least 5×10^{51} erg. In Figure 11, we plot the filtered and unfiltered absolute magnitude light curves of CSS100217 along with that of the Type IIn supernova 2006gy (Smith et al. 2007). Considering the difference absolute luminosity between these two events ($\delta R > 1$ mag), the approximate factor of two difference in energy appears as expected.

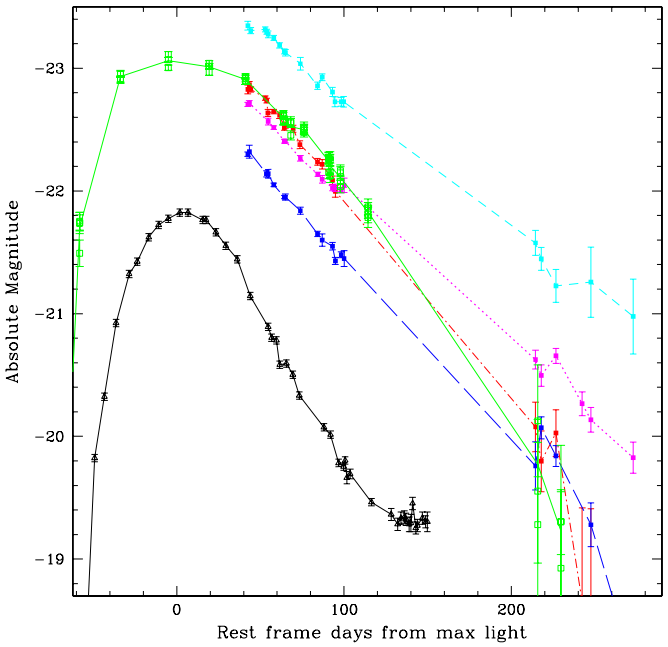

Figure 11. Light curve of CSS100217. Here, we show the luminosity of transient event CSS100217 compared to the luminous and energetic Type IIn SN 2006gy from Smith et al. (2007; open triangles). The CSS100217 light curves are given for V_{CSS}, solid line with open boxes; I short-dashed line; R dot-dashed line; V dotted-line; and B long-dashed line. The maximum brightness occurred at MJD = 55250 which corresponds to ∼6 days after discovery. See the text for further details.

(A color version of this figure is available in the online journal.)

3.4. High-resolution Imaging

In order to discern whether CSS100217 was due to an event occurring in the nucleus of SDSS J102912.58+404219.7, as required for a TDE or other AGN variability, we investigated the location of the event. First, we determined the location of the flux in the difference images relative to the centroid of SDSS J102912.58+404219.7. Such astrometry can be used to disambiguate variable sources that are not resolved because of blending or high background light (Nelson et al. 2009). A significant offset between the two centroids would very strongly suggest that the object was a supernova. By stacking the sequence of difference images we found that the additional flux was within 0.″3 of the galaxy's nucleus. In order to check this result we undertook follow-up observations with the Large Binocular Telescope plus LUCIFER near-IR camera and spectrograph. No second source was resolved in our K_s-band images with resolution of 0.″4.

To obtain a higher level of precision, and possibly separate the source for the AGN, we obtained *HST* Director's Discretionary Time with the *HST* WFC3. We obtained WFC3 images in F390W, F555W, and F763M filters spanning one orbit. The filters were chosen to separate the blue continuum and H_α components of the spectra, since we expected a Type IIn supernova would be a strong source of H_α and this might enable a clearer separation from the hot blue central AGN. A customized seven-pointing dither was chosen in each band to maximize the subsampling of the *HST* PSF (Anderson & King 2000).

In Figure 12, we show a co-added SDSS image of the host galaxy along with the dithered *HST* WFC3 F555W image of the host including transient CSS100217. The SDSS pre-event co-add consists of the median of 15 images (u,g,r,i,z) of the galaxy observed on three nights (2002 December 31, twice, and 2003 March 26), whereas the *HST* image is derived from seven dithered images. The SDSS and *HST* observations show that the galaxy is completely dominated by the central nucleus with no clear sign of extension of the host galaxy. Subtraction of *HST* PSF models did not reveal the galaxy or any sign of a second separated source. In comparison, Deo et al. (2006) examined *HST* data for a sample of 87 Seyfert galaxies and found almost all occurred in clear spiral galaxies. Only two objects appeared point-like (HEAO 2106-099 and Mrk 335). However, Bentz et al. (2009) examined *HST* data for 35 AGNs, including Mrk 335, and were able to fit the faint host galaxies for all. It is therefore likely that the host galaxy simply has a very low surface brightness relative to the nucleus.

We obtained images of the object using the NIRC2 imager and laser guide-star adaptive optics (Wizinowich et al. 2006) at the Keck II 10 m telescope on Mauna Kea, Hawaii, on 2010 June 3 UT. We used the K' band and obtained multiple dithered exposures both in the NIRC2 "wide field" mode, with a sampling of 40 mas pixel^{-1}, and the "narrow field" mode, with a sampling

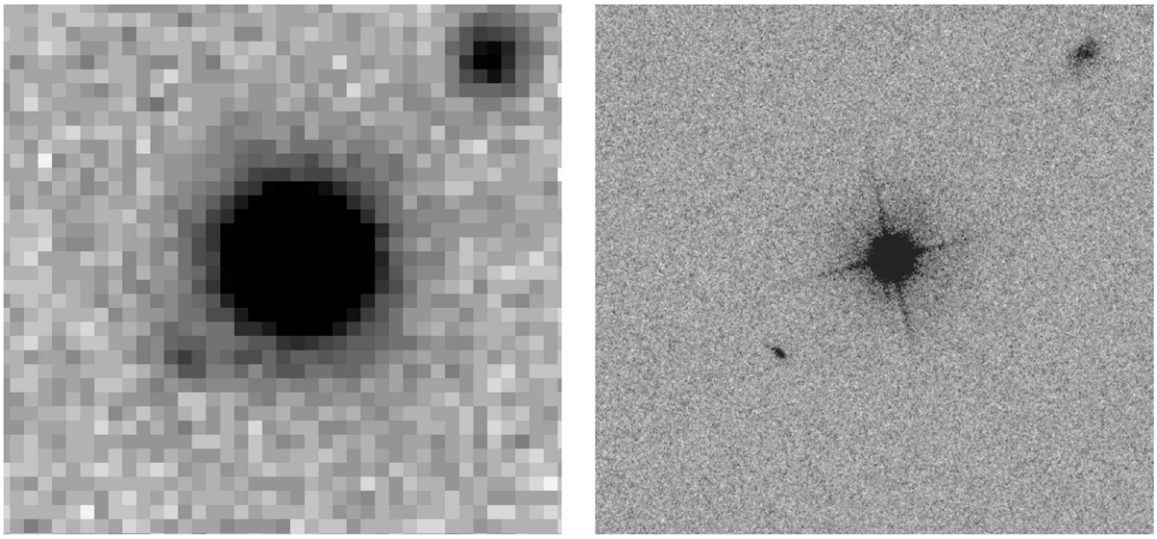

Figure 12. SDSS image of the host galaxy of CSS100217, SDSS J102912.58+404219.7 (left) and *HST* F555W image of the event during outburst (right). The images are 15.″5 across with north up and east to the left.

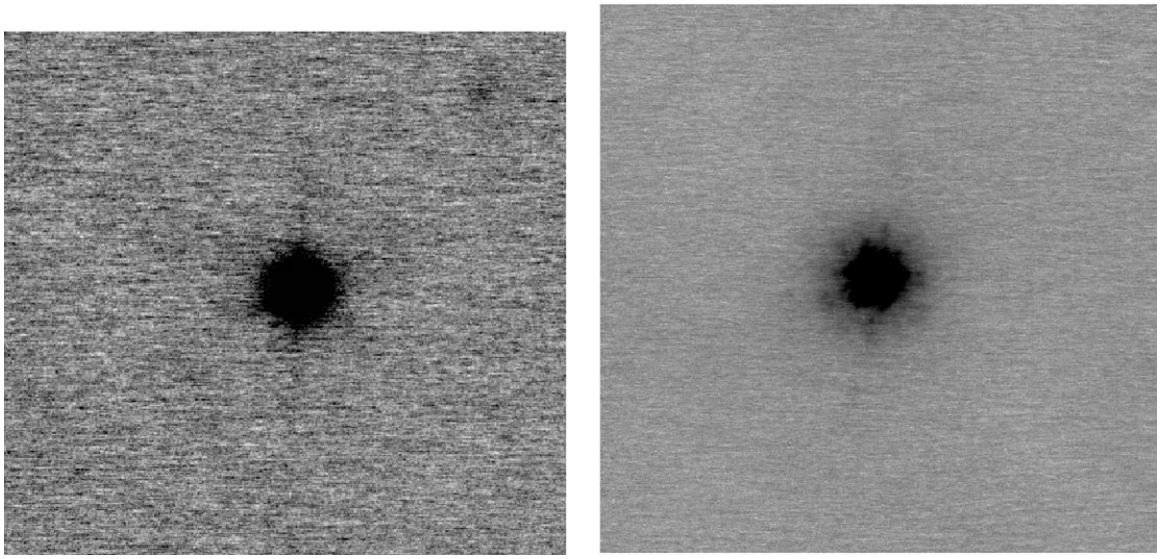

Figure 13. Keck NIRC2 images of CSS100217 with north up and east to the left. Left: the "wide field" image with scale ∼15″ across. Right: the "narrow field" image with scale ∼10″ across.

of 10 mas pixel^{-1}, followed by observations of a nearby bright star to define the PSF. For our tip-tilt configurations and seeing conditions, the estimated K'-band Strehl ratio is ∼0.2. A co-add of a number of dithered images is shown in Figure 13. At the redshift of the transient, the pixel sizes correspond to projected linear sizes of ∼103 and ∼26 pc. Thus, the effective angular resolution of these observations is comparable to or slightly better than that of the *HST* images, and the source appears unresolved even with the higher resolution images.

3.5. Radio Observations

3.5.1. EVLA

We observed CSS100217 with the Expanded Very Large Array (EVLA) for three separate epochs between 2010 April and May. Each observation was 1 hr in duration. We observed simultaneously at central frequencies of 4496 MHz and 7916 MHz using the new wide *C*-band feeds for a total bandwidth of 256 MHz. The EVLA was in the compact D configuration, yielding synthesized beams of 13″ and 7.″5 at 4496 MHz and 7916 MHz, respectively. Phase calibration was carried out by making short observations of the nearby point source J1033+4166 every 10 minutes, while amplitude and bandpass calibration was achieved using an observation of 3C 147 at the end of each observing run. The data were reduced following standard practice in the Astronomical Image Processing System (AIPS) software package.

Table 7
EVLA Radio Measurements

2010 UT Date	Flux 4.5 GHz (μJy)	Flux 7.9 GHz (μJy)	α
Apr 29.22	447 ± 26	399 ± 24	−0.20 ± 0.02
May 14.07	312 ± 24	349 ± 24	+0.19 ± 0.02
Jun 01.05	408 ± 16	506 ± 28	+0.38 ± 0.03

A single, unresolved radio source was detected on all three epochs. Table 7 summarizes the results of these observations. The flux density varied between 0.3 and 0.5 mJy, but the spectrum was relatively flat between these two radio frequencies.

Inspection of the archival FIRST images made with data taken in the early 1990s (Becker et al. 1995) shows a possible detection at this position with a 1.4 GHz flux density of 300 ± 145 μJy. At the redshift of $z = 0.15$ ($d_L = 705$ Mpc), these flux densities correspond to a spectral luminosity $L_R \simeq 2.3 \times 10^{29}$ erg s^{-1} Hz^{-1}. The variation in spectral index of the 4.5 GHz and 7.9 GHz data suggests that the distribution is getting flatter and eventually inverting. The origin of this effect is unknown.

The radio luminosity of CSS100217 plus the host galaxy exceeds that of the most luminous Type Ib/c and II supernovae by factors of several (Chevalier et al. 2006) and is approaching values more typical of GRB afterglows. The absolute near-IR luminosity from 2MASS is $M_K = -24.65$. Mauch & Sadler (2007) studied the properties of star-forming galaxies and radio-loud AGNs. The combination of the 2MASS K-band luminosity and initial FIRST radio power places the object in the region of overlap between both star-forming galaxies and AGNs. Based on the local luminosity function star-forming galaxies are slightly more common at this radio power (Mauch & Sadler 2007). However, during outburst the near-IR luminosity is $M_k = -26$, making it brighter than most star-forming radio galaxies. Additionally, when considered with the flat spectral index and the modest variability, the simplest explanation is that the radio emission originates from nuclear activity from the central black hole in the galaxy.

3.5.2. GMRT

The source CSS100217 was observed with the Giant Meterwave Radio Telescope (GMRT) on 2010 May 23 at a center frequency of 608 MHz. Data were recorded using a new software correlator with a bandwidth of 33 MHz divided into 512 channels. The total observing time was 5 hr (including the calibration overheads). A total of 2 hr 45 minutes was spent on the target, interspersed with 4.5 minute scans on the phase calibrator every 45 minutes. The source 0834+555, which is an unresolved point source at 610 MHz, was chosen as the phase calibrator, while 3C 147 and 3C 286 were used to calibrate the flux as well as the bandpass. Their fluxes were determined using the Baars et al. (1977) flux scale. Data were reduced using standard AIPS processing.

The image was made using the central 30.5 MHz centered at 607.95 MHz. The synthesized beam achieved was $5\farcs78 \times 4\farcs21$. An unresolved point source of flux 873 ± 80 μJy was detected. The rms near to the source was about 50 μJy, which implies a detection significance of about 17σ. The combination of EVLA data with GMRT suggests a spectral slope α between −0.4 and −0.5 depending on EVLA observation date. This is similar to values commonly observed in low-luminosity Seyfert galaxies (Ulvestad & Ho 2001).

3.6. X-ray Observations

X-ray observations of the transient were taken on 2010 April 6 with the *Swift* X-Ray Telescope (0.2–10 keV) to determine whether the object was a strong soft X-ray source as expected for a TDE. The object was clearly detected with flux $\sim 10^{43}$ erg s^{-1} and is a soft source consistent with a TDE or an NLS1 galaxy (Boller et al. 1996).

3.7. Fermi-LAT Follow-up

We searched for emission in the gamma-ray band that was spatially and temporally coincident with the optical flare from CSS100217 using data from the Large Area Telescope (LAT) aboard the *Fermi Gamma-ray Space Telescope* satellite. The *Fermi*-LAT instrument is sensitive to gamma-ray photons with energies in the range 20 MeV to >300 GeV. With its ∼2.4 sr field of view (FoV) and scanning mode of operation, *Fermi*-LAT provides all-sky monitoring coverage on 3 hr timescales (Atwood et al. 2009).

We extracted data within a 20° acceptance cone centered on the CSS100217 position during the period 2009 November 20 to 2010 July 4, covering the nominal duration of the outburst. We analyzed these data using the standard *Fermi*-LAT data analysis software, running the unbinned maximum likelihood analysis tasks; we fit the data over 1 week intervals and over the entire extraction period. (See Abdo et al. 2010a for descriptions of the fitting methods.) The source model for these analyses comprised a power-law point source at the CSS100217 position (with unconstrained photon index and normalization), all point sources from the 1FGL catalog (Abdo et al. 2010a) within the data extraction region, and the models for the Galactic (`gll_iem_v02.fit`) and isotropic diffuse emission (`isotropic_iem_v02.fit`) that were recommended by the *Fermi*-LAT team. The software and diffuse files are available from the *Fermi* Science Support Center (http://fermi.gsfc.nasa.gov/ssc/). The flux normalizations of the Galactic and isotropic components, the point sources within 5° of CSS100217, and the flaring blazar Mrk 421, which is 7°.25 from CSS100217, were allowed to be fit freely. All other point-source parameters were held fixed at their 1FGL catalog values. No evidence for a point source at the location of CSS100217 was found in the full data set or in any of the 1 week intervals. The 95% confidence limit (CL) flux upper limit in the energy band 100 MeV to 100 GeV for the full data set is 3.1×10^{-8} photons cm^{-2} s^{-1}. For the 1 week intervals, the 95% CL upper limits ranged from 1.1×10^{-7} to 3.4×10^{-7} photons cm^{-2} s^{-1}. Near the time of the peak optical flux (MJD 55272), the 1 week 95% CL upper limit for CSS100217 was 2.1×10^{-7} photons cm^{-2} s^{-1}. We note that the two nearest point sources, 1FGL J1033.2+4116 (0°.95 offset from CSS100217) and 1FGL J1023.6+3937 (1°.52 offset), are both associated with blazars (Abdo et al. 2010b). Neither source showed significant emission during any of the weekly time intervals that we considered, and the fitted fluxes for each were $<6 \times 10^{-8}$ photons cm^{-2} s^{-1} at the time of the peak optical flux of CSS100217.

Since luminous optical transients such as Type Ib/c supernovae have been associated with GRBs (Paczynski 1997; Stanek et al. 2003), we considered the possibility that CSS100217 was associated with such an event. We queried the GCN Notices archive (http://gcn.gsfc.nasa.gov/) for any bursts that occurred around the time of the onset of the optical flare. From 2009 November 20 to December 29, GCN Notices for 49 GRB triggers were issued. Of those 49 triggers, the closest GCN location to CSS100217 was 14°.6 away (R.A., decl. = 155°.667, 55°.233, J2000) for trigger number 281250934 issued by the Gamma-ray Burst Monitor (GBM) aboard *Fermi* with trigger time 05:15:32.98 UT, 2009 November 30. The other 48 GRB candidate locations were more than 20° away from CSS100217. No obvious transient at the CSS10027 location is present in the LAT data stream in the 200 s bracketing the GBM trigger time. However, at the time of the trigger, the GBM location was at the edge of the LAT FoV (off-axis angle of 70°). So to search for possible extended, longer timescale emission (e.g., Abdo et al. 2009), we extracted data centered on the CSS100217 position for the 10^4 s following the GBM trigger. An unbinned

likelihood analysis of those data finds no evidence for a point source and yields a 95% CL flux upper limit of 3.7×10^{-6} photons cm^{-2} s^{-1} for energies 100 MeV to 100 GeV.

4. THE NATURE OF THE TRANSIENT CSS100217

Determination of the nature of the transient CSS100217 bares distinct similarities to that of the transient SDSS J095209.56+214313.3 discovered by Komossa et al. (2008). Following the initial interpretation of SDSS J09522.56+2143 as a TDE by Komossa et al. (2009) obtained additional data and reinterpreted their discovery as either a TDE, AGN variability, or a luminous Type IIn supernova. In this case we have the same three likely causes for the observed outburst. However, unlike SDSS J095209.56+214313.3, which was only discovered and followed 2 years after the outburst, we obtain a spectrum before the event and were aware of the distinctive nature of the event from well before it reached its optical peak. We were thus able to obtain significant data covering the event. Nevertheless, the interpretation of CSS100217 remains unclear. Below we will outline the cases for and against each of the possibilities.

4.1. Type IIn Supernovae

As noted above CSS100217 bares distinct similarities to Type IIn supernova explosions. Therefore it is useful to compare the event to known sources of this type. Type IIn supernovae are known to have a 5 mag range in their peak brightness and outburst timescales from months to years (Richardson et al. 2002). In recent years luminous and energetic Type IIn supernova, such as SN 2006gy (Quimby et al. 2006), have been discovered and analyzed (Smith et al. 2007). Comparison between the light curve of CSS100217, and the energetic Type IIn supernova 2006gy (Smith et al. 2007) is given in Figure 11. The similarity of these curves suggests a possible relation between the two events. Additional Type IIn supernova with very long timescales have also been recently discovered. For example, SN 2008iy (Catelan et al. 2009) and 2003ma (Rest et al. 2011) have been observed over many years. The decline rate measured from our difference image photometry for CSS100217 at late times is 0.0175 mag day^{-1}. This is much faster than observed for the longest events, but slower than observed for most Type IIn supernovae.

Additionally, the spectra of CSS100217 show evolution of the broad Balmer components. In the initial IGO spectrum the H_α component had FWHM $\sim$ 2800 km s^{-1} and 3 months later during the Keck observations the width was $\sim$4800 km s^{-1}. This is close to that observed for H_α in SN 2006gy which initially had FWHM = 2500 km s^{-1} and later 4000 km s^{-1} (Smith et al. 2007). The H_β emission shows the similar evolution. In the case of CSS100217, as in known Type IIn supernovae, we see that the H_α emission component strengthens with time, while the observed luminosity declines. This suggests that the emission will continue for an extended period of time. The spectrum of CSS100217 exhibits relatively strong high-energy Balmer lines (Hγ, Hδ, Hϵ) that are more commonly observed in luminous blue variable (LBV) outbursts like SN 2009ip (Smith et al. 2010b). This may be attributed to the surrounding medium being hotter than normally observed for Type IIn supernovae. The emission features observed in Type IIn supernovae are due to the expansion of explosion ejecta into a dense circumstellar medium (CSM) surrounding massive eta Carina-like stars (Smith et al. 2010a). In such cases, the outbursts of LBVs in years prior to the explosion are believed to cause massive shells through which the blast shock travels. The location of the event near the AGN may be responsible for causing additional heating of the CSM surrounding a massive progenitor star.

4.1.1. Supernovae in Nuclear Regions

Modern optical searches for supernovae have been tuned to avoid events occurring near galactic nuclei. The main reason for this is the high likelihood that such variability is due to variation caused by an AGN. AGNs are thought to be present in 43% of galaxies (Ho et al. 1997). Therefore, the chance of finding a variation in any given galaxy due to an AGN may be larger than the chance that this is due to a nuclear supernova. In addition, supernovae lying far from the crowded cores of galaxies can also be more readily discovered and spectroscopically confirmed. Furthermore, supernovae in the dense cores of regular galaxies are likely to suffer from significant extinction ($A_V > 10$ in many cases), so that few are visible in optical wavelengths. However, in the cores of luminous infrared galaxies, such as the interacting system Arp299, at least one CCSN is expected every year (Mattila et al. 2004). Such supernovae can be discovered using near-IR imaging or radio observations (Perez-Torres et al. 2007).

Perez-Torres et al. (2007) discovered 26 sources that they believed to be radio supernovae or supernova remnants within the central 150 pc of Arp299A. Additional follow-up by Perez-Torres et al. (2010) showed that one of the central sources was in fact a low-luminosity AGN. However, Perez-Torres et al. (2010) identified one companion source within a projected separation of 2 pc as a radio supernova. In many cases, the supernova observed near the core of a galaxy will lie in front of the dust extinction layer making them visible in optical surveys. Additionally, supernova lying within the narrow-line region near an AGN (10 pc to 1 kpc) may not be obscured by the dense gas and dust disk. Botticella et al. (2008) identified 28 supernova candidates lying with 0.″5 of the core of their host galaxies. Of these only 50% were attributed to AGNs based on their long timescale variability.

Strubbe & Quataert (2010) studied how one could discern nuclear supernovae from TDEs. They found that *HST* or ground-based adaptive optics were needed to reduce contamination of supernovae near the galactic nucleus to a level close to that expected for TDEs. However, even with high-resolution imaging the number of Type Ia and II supernovae will exceed the number of TDEs.

4.2. Tidal Disruption Events

The search for TDEs has recently led to the discovery of a number of candidate TDEs (Komossa et al. 2002; Esquej et al. 2007; Gezari et al. 2009a; Cappelluti et al. 2009; Maksym et al. 2010). Dynamical models of galaxy nuclei predict that these events should occur at a rate of 10^{-4} to 10^{-5} galaxy^{-1} yr^{-1} (Magorrian & Tremaine 1999; Wang & Merritt 2004). In comparison these events are 100 times less commonly observed than supernovae, but still within the range of transient surveys such as CRTS, PTF, PanSTARRS, and LSST.

The signature of such events is bright UV and soft X-ray emission from the high-temperature outburst event that occurs as the star is shredded and accreted by a massive black hole. Models for the optical light curves of these events show significant variation with black hole mass. TDEs are expected to have temperatures of $\sim 10^5$ K and a luminosity that declines with time as $t^{-5/3}$. However, recent detailed models for the light curves of these events by Strubbe & Quataert (2009) and Lodato & Rossi (2011) found the optical and UV light curve to be significantly

shallower than $t^{-5/3}$. Lodato & Rossi (2011) find a very slow $t^{-5/12}$ decline at late times.

Although the clearest signature for TDEs is a flare near the center of an otherwise dormant galaxy, such events are very likely to occur in galaxies that exhibit significant nuclear activity from black holes in the right mass range. In particular, supermassive black holes seen in blazars and QSOs are thought to be too massive for such disruption events to occur (Hills 1975). Instead, in these cases the stars are swallowed whole. For black holes with masses $<10^8\ M_\odot$, as in Seyfert galaxies, such events should occur. Clearly the presence of X-ray, UV, and radio variability in AGNs make the discovery of TDEs associated with AGNs a much more complex task.

The slow rise and decline of the optical light curve of CSS100217 is inconsistent with the $t^{-5/3}$ decline expected for TDEs (Komossa et al. 1999) as well as the more recently theorized $t^{-5/12}$ dependence. A continuum fit to the IGO spectrum shifted to rest gives a temperature of $(1.6 \pm 0.2) \times 10^4$ K, much lower than the expected TDE value of $\sim 10^5$ K. As noted earlier, the NUV photometry taken on 2010 January 29 by *GALEX* gives $NUV = 17.08$. This value is 1.9 mag brighter than when observed on 2004 January 24 (Gezari et al. 2010). At this time the object was ∼1.5 mag brighter in CSS observations. The combination of extinction-corrected *GALEX* NUV flux (centered at 2315 Å) along with the IGO data is consistent with a temperature of $\sim 10^4$ K. However, this early temperature is poorly constrained because of the 3 week period between these observations.

Recently, Strubbe & Quataert (2010) studied the spectroscopic signatures of TDE events. The results suggest that most events will give rise to featureless blackbody spectra at wavelengths above 2000 Å. In an otherwise inactive galaxy the signature of a disruption event by a quiescent black hole would be similar to the early spectrum of a supernova. However, the strong spectroscopic features would not evolve as time passed. In the presence of an AGN the combination of a featureless spectrum with that of the AGN would be very difficult to discern from that of just an AGN. Strubbe & Quataert (2010) note that TDEs, unlike Type IIn supernovae, become hotter with time and are not expected to produce strong optical emission lines. The theoretical predictions for spectra, temperature, and variability all appear inconsistent with the observations of CSS100217.

4.3. AGN Variability

As the host galaxy appears to contain an AGN, it is important to consider whether CSS100217 might be due to an accretion event involving the massive black hole. In the previous section we determined that the event was very unlikely to be due to the tidal disruption of a star by the black hole. However, as AGNs are by nature variable it is necessary to understand the limits of this variability in comparison to CSS100217. Recently, Ai et al. (2010) investigated the variability of a small sample of 58 narrow-line Seyfert-1s (NLS1s) and 217 broad-line Seyfert-1s (BLS1s). They found that the variability in 3 years of SDSS stripe-82 data was less than 0.4 mag. As the host galaxy for CSS100217 is an NLS1, the sample of Ai et al. (2010) is too small for a meaningful understanding of the true limits of variability in NLS1s.

4.3.1. Comparison of CSS100217 with Known NLS1

In order to assess how the variability we observed in CSS100217 matches with that naturally observed for NLS1-type AGNs, we decided to investigate the light curves of a large, uniform sample of spectroscopically confirmed NLS1 galaxies. We first selected the spectroscopically confirmed sample of NLS1 from Zhou et al. (2006). This set consists of ∼2000 NLS1, chosen from emission-line galaxies in the SDSS dr5 catalog. We found matches to most of the Zhou et al. NLS1s in the CSS data archive and for each object we extracted the photometry from the same 5 year period as CSS100217. Many of the light curves show clear, significant variation over this period.

After removing the NLS1 light curves that were affected by blends or bad photometry (due to being on image edges, etc.), we were left with 1541 objects. We matched the objects against the FIRST radio catalog using a 5″ radius. Of the 143 matches, only 3 had an offset larger than 2″. The NLS1 host of CSS100217 was not detected by FIRST or NVSS radio surveys.

For each light curve we iteratively determined the mean and range of values for the 90% of data lying nearest the mean. This process removes photometric outliers due to bad photometry caused by artifacts, satellite trails, bad seeing, etc. We then calculate the standard deviation assuming that the remaining data follows the normal distribution. In Figure 14, we plot the scatter of the data points for the NLS1 sample. As the scatter is dominated by increasing photometric uncertainty with decreasing brightness we also plot the data after removing this trend. Clearly CSS100217 is an extreme outlier, whether we correct for the photometric uncertainty trend or not.

To further investigate the variability we determined the median magnitude for each light curve and the value that varies most from the median in terms of photometric uncertainties. Here, we included only those data points lying within $\pm 3\sigma$ as determined from the scatter in each light curve. This sigma cut was necessary because of outliers in other NLS1 photometry, due to artifacts, etc. In Figure 15, we plot the peak variation versus the number of sigma that the point represents. The size of the deviations are mainly less than 5σ, suggesting that the photometric uncertainties are approximately correct. We also show the result when we have removed the effect of increasing photometric scatter with increasing magnitude. This figure shows that CSS100217 is once again an extreme outlier in both plots. As the host of CSS100217 is brighter than most of the NLS1 sample, the offset is most clearly seen in the corrected plots. We note that the largest deviation (ΔV) from the median is not shown in the figures for CSS100217 as the true maximum lies $>3\sigma$ from the median magnitude. The level of observed NLS1 variation is consistent with that found by Ai et al. (2010).

Among the Zhou et al. (2006) spectroscopically selected NLS1 two are known to exhibit significant variability on short timescales. However, both of these NLS1, SDSS J150506.47+032630.8 (QSO B1502+036, Yuan et al. 2008) and SDSS J094857.3+002225.5 (Zhou et al. 2003), are radio-loud NLS1 (380.49 mJy and 111.46 mJy, respectively in FIRST data). In Figure 16, we present the light curves of these two NLS1. Both objects exhibit erratic variability which is completely unlike CSS100217 or the other radio-quiet NLS1 examined. In these cases, like BL Lacs, the variability has been attributed to a jet lying along our line of sight and emanating from the central black hole. The optical variability is attributed largely to this source. The maximum observed variability for these objects in CSS data of SDSS J150506.47+032630.8 and SDSS J094857.3+002225 is ∼1.5 and ∼1.2 mag, respectively. The CSS light curves of these NLS1 resemble those of blazars monitored by CRTS. SDSS J094857.3+002225 exhibits intra-day variability (Liu et al. 2010). These two sources are ∼500 times

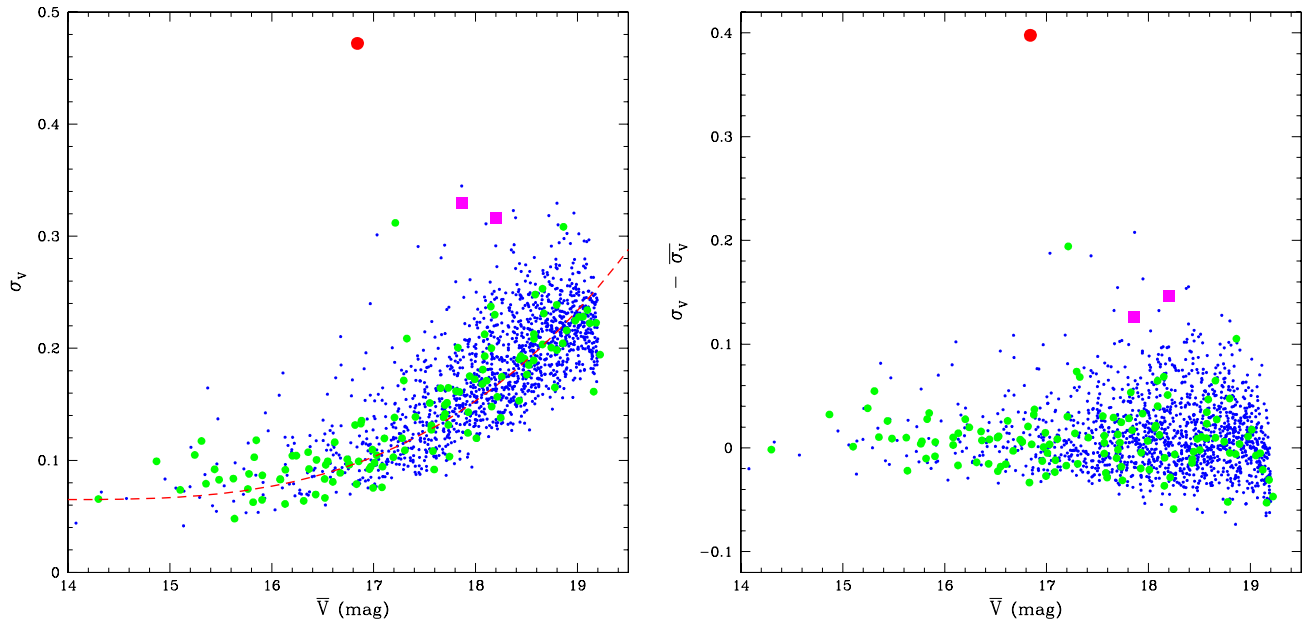

Figure 14. Comparison of the variability of CSS100217 (large dot) with known NLS1s selected from Zhou et al. (2006). Radio sources detected by FIRST are marked with medium-size dots. The location of radio-loud NLS1 SDSS J150506.47+032630.8 and SDSS J094857.3+002225.5 is marked with boxes. Left: standard deviation of the light curve based on central 90% of the data. The dotted line shows the trend of increasing scatter that is mainly due to decreasing brightness. Right: the scatter of the data after removing the trend of increasing scatter with decreasing magnitude.

(A color version of this figure is available in the online journal.)

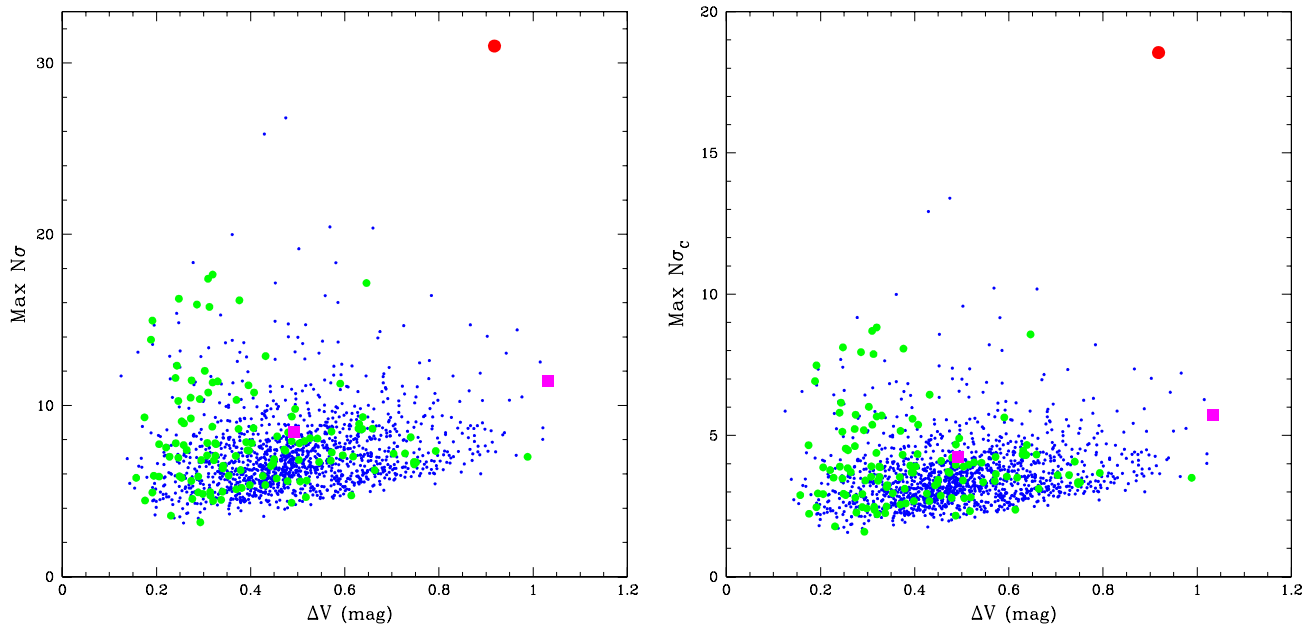

Figure 15. Variability of CSS100217 (large dot) relative to known NLS1s selected from Zhou et al. (2006). Radio sources detected by FIRST are marked with medium-size dots. The location of radio-loud NLS1 SDSS J150506.47+032630.8 and SDSS J094857.3+002225.5 is marked with boxes. Left: maximum deviation from median magnitude in terms of sigma based on NLS1 data. Right: maximum deviation from median magnitude in sigma based on NLS1 data that has been corrected for increasing scatter with decreasing brightness.

(A color version of this figure is available in the online journal.)

brighter than CSS100217 at radio wavelengths and neither exhibits a prolonged outburst like that observed for CSS100217.

From our analysis we find that a small fraction of the NLS1 exhibit significant variability. In most cases the variability is a slow change in brightness over a timescale of years, as previously observed for QSOs. A couple of NLS1 in our large sample exhibit a high level of variability but none like that observed in CSS100217. In the cases where a rapid event lasting months is seen, the source is consistent with a luminous supernova. This strongly suggests that CSS100217 is not due to regular AGN variability. However, it is not possible to completely exclude very rare sources of AGN variability. Recent reports of AGN outbursts have been made in sparsely sampled data by Kankare et al. (2010) and Valenti et al. (2010). However, these have been found to be due to gradual changes rather than outbursts when examined in better sampled data (Drake et al. 2010b, 2010c). TDEs themselves are examples of rare AGN outbursts. Although the characteristics of CSS100217 do not

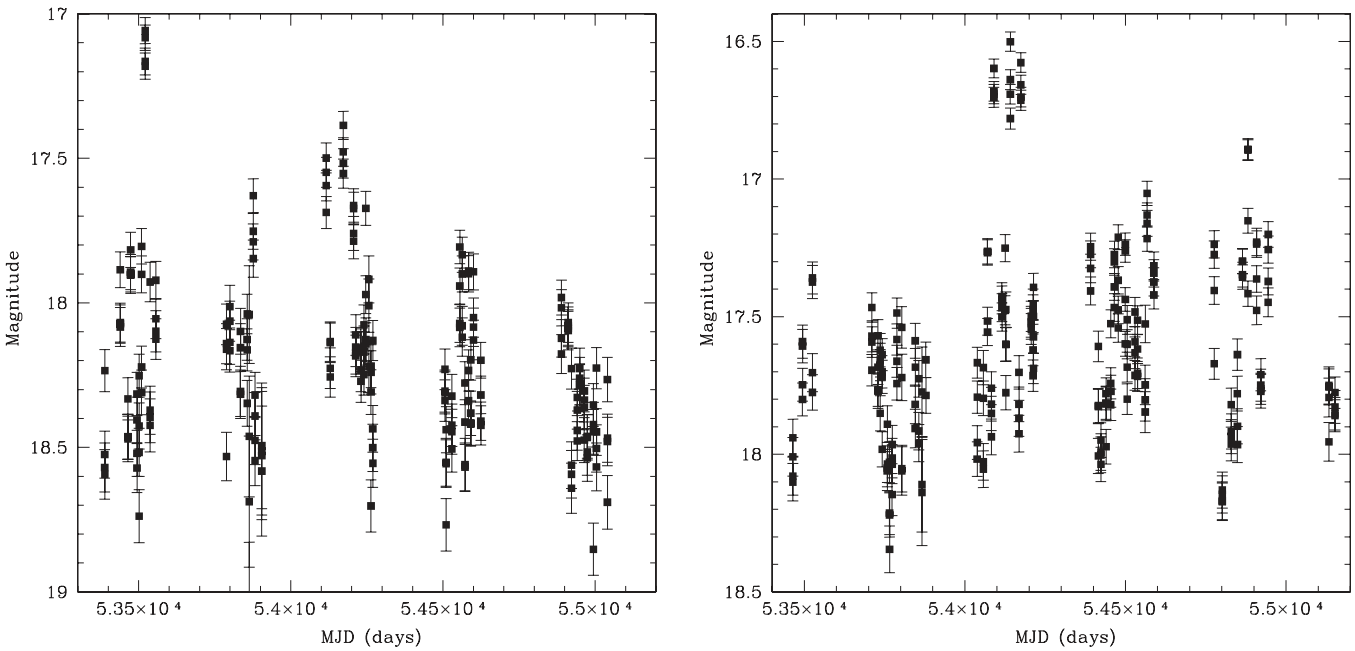

Figure 16. CSS *V*-band light curves of two highly variable radio-loud NLS1 galaxies. Left: the light curve of SDSS J150506.47+032630.8. Right: the light curve of SDSS J094857.3+002225.5.

follow current theoretical predictions for TDEs, recent revisions of both the timescale (Lodato & Rossi 2011) and spectroscopic signature of such events (Strubbe & Quataert 2010) suggest a need for constraints based on empirical data. Future surveys such as LSST should provide these constraints.

5. DISCUSSION AND CONCLUSIONS

We have analyzed the multi-wavelength data covering the discovery of the unusual transient CSS100217. The coincidence of the event's location with an NLS1 galaxy makes the event most consistent with a TDE, AGN variability, or a supernova.

5.1. CSS100217 as a TDE

The large outburst of CSS100217 within 150 pc of the nucleus of an AGN make it a good candidate for the tidal disruption of a massive star by the central black hole. The object is also detected as an X-ray source in *Swift* telescope follow-up. However, the event exhibits a slow rise over a period of months and a similarly slow decline. The light curve is completely inconsistent with theoretical TDE models that predict an immediate rise and $t^{-5/3}$ decline. However, the more recent light curve models for TDEs (Lodato & Rossi 2011) show optical light curves with rise times of a month followed by a flat peak and much slower decline following $t^{-5/12}$. Such light curves are very similar to those observed for supernovae, although with much longer tails. The peak brightness $M_{V\,\mathrm{CSS}} \sim -23$ of the event is far greater than theorized for TDEs, which are predicted to reach the brightness of regular supernovae $M_V \sim -18$. Furthermore, the galaxy-subtracted spectra of the event exhibit strong Balmer emission and a continuum consistent with $T = 1.5 \times 10^4$ K rather than the theorized 10^5 K value. Based on theoretical predictions CSS100217 is a poor TDE candidate.

5.2. CSS100217 as AGN Variability

The host galaxy spectrum of SDSS J102912.58+404219.7 exhibits both broad and narrow Balmer lines as well as Fe II, consistent with this being an NLS1 galaxy. The *HST* follow-up of the event shows that the location of CSS100217 is consistent with the location of the bright nucleus. The object is also found to be an X-ray source in *Swift* data, a radio source in EVLA and GMRT follow-up observations, and is brighter than known supernovae at these wavelengths.

It is well known that AGN variability can amount to variations of a magnitude or more over the period of a number of years. As AGNs are more common than supernovae, surveys for supernovae specifically avoid follow-up of detections occurring near the cores of galaxies. Indeed, the IAU recommend that all supernova candidates are checked against the Véron-Cetty and Véron (2010) AGN catalog before submission. Events near the core of galaxies are not announced or given an official ID by the IAU's Central Bureau for Astronomical Telegrams unless they are also spectroscopically confirmed to reduce the possibility that any given discovery is due to AGN variability. The peak outburst luminosity of CSS100217 is well within the range observed for NLS1. One model for AGN variability suggests that the cause is the superposition of supernova explosions in giant stellar clusters (Trelevich et al. 1992). In this model the explosions interact with the high-density circumnuclear environment. If this model is correct, CSS100217 could be an example of such an event.

Analysis of host galaxy SDSS J102912.58+404219.7 on the BPT diagram suggests that it is not a typical NLS1. The object lies on the locus of starburst galaxies suggesting that the galaxy is also undergoing rapid star formation. Comparison of the optical variability of CSS100217 with 1500 other NLS1 galaxies selected from SDSS data strongly suggests that the observed variability is inconsistent with normal AGN variability. The follow-up spectra of CSS100217 exhibits a Balmer component that is significantly broader than the archival spectrum. This component is twice as broad as the $\sim$2000 km s^{-1} defining limit for NLS1 galaxies (Osterbrock & Pogge 1985). Furthermore, although the narrow and medium H_α velocity components vary little in width with time, the strength increased as the event

faded rather than decreasing. Variation of the narrow component on short timescales is not expected because of the size of the narrow-line region. The event also shows the presence of a hot continuum component not observed in the prior SDSS spectrum. This component cools as the outburst fades. Furthermore, although there are few examples of supernova occurring near the cores of AGNs, this is due to active selection against such events because of possible AGN variability. Similar events may have been detected in the past but dismissed because of their location near the core of a galaxy and the presence of an NLS1-like spectrum. Based on the observations of NLS1, CSS100217 is unlikely to be due to AGN variability.

5.3. CSS100217 as a Supernova

The distinctive smooth rise and fall of the light curve of CSS100217 closely matches the general shapes observed for supernovae and Type IIn, such as SN 2008iy and SN 2006gy. Spectroscopic follow-up of CSS100217 reveals strong narrow Balmer features superimposed on broader features as is required for classification of Type IIn supernovae. The Balmer features are observed to vary significantly from that observed in SDSS spectrum. Some variation in the broad-line strength is expected for NLS1 galaxies but such rapid variation in the narrow-line strength has not been observed. Additionally the follow-up spectra exhibit a broader, 4000 km s^{-1} component that is not seen in the SDSS spectra. The velocity of this component increases with time in both H_α and H_β until the most recent observations while the narrow and medium components shows little change. Also, the strength of the broad component is seen to increase even as the event fades. The host-subtracted spectrum exhibits strong Fe II lines. Such lines are pronounced in both NLS1 spectra and supernova Type IIn like SN 2008iy, SN 2007rt (Trundle et al. 2009) and SN 1997ab (Hagen et al. 1997). Such lines are not predicted by current models of TDEs.

As is characteristic of Type IIn (Trundle et al. 2009) the spectra of CSS100217 do not exhibit the broad P-Cygni features commonly observed in other Type II supernova. For example, the Type IIn prototype, SN 1998Z was determined not to exhibit a P-Cygni absorption component (Turatto et al. 1993). Narrow P-Cygni features are commonly observed in high-resolution data of Type IIn supernova, but are not seen in low-resolution data (Trundle et al. 2009). In Figure 17, we contrast the spectrum of CSS100217 with that of SN 2008iy.

The temperature derived from the continuum in the initial follow-up spectrum ($T = 1.5 \times 10^4$ K) is consistent with supernovae in general and very similar to that observed for the luminous Type IIn SN 2006gy (Smith et al. 2007). The brightness of this event, $M_V = -22.7$, is the greater as observed for past IIn supernovae SN 2008fz (Drake et al. 2010a) and SN 2008es (Gezari et al. 2009b). As Type IIn supernova are known to exhibit a variation in peak brightness of at least 5 mag, this discovery is not very surprising, particularly since the most luminous among these supernovae have only been discovered in the past decade as surveys have begun which search for transients in intrinsically faint galaxies (Drake et al. 2009).

The presence of a luminous supernova near the core of an AGN is expected to be a rare occurrence. However, the host spectrum suggests a significant star formation rate, which would enhance the rate of Type II supernova—as seen in Arp299A by Perez-Torres et al. (2007). Additionally, based on Strubbe & Quataert (2010), the rate of Type II nuclear supernovae will exceed the rate of TDEs by a factor of ~3 at 0.″05 resolution for a 10^7 $M_\odot$ black hole. The radio detections by GMRT and EVLA

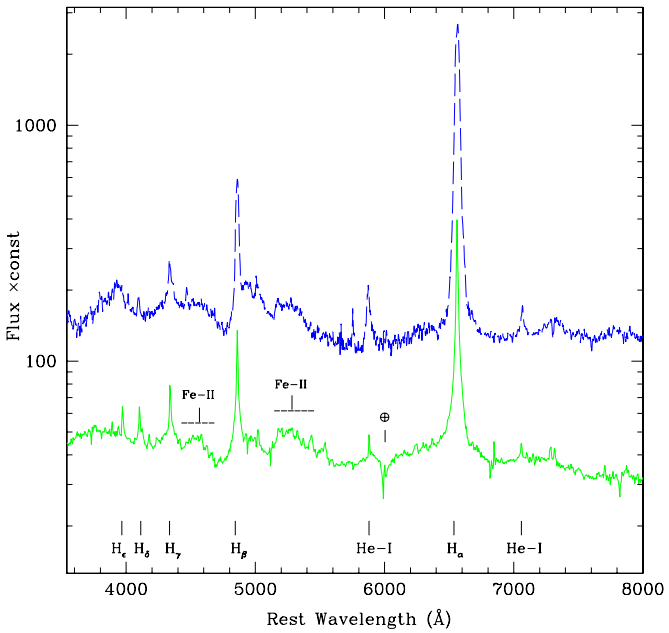

Figure 17. Comparison between the host-subtracted Keck spectrum of CSS100217 and that of Type IIn supernova SN 2008iy. Solid line shows the spectrum of CSS100217. Long-dashed line shows the spectrum of SN 2008iy. In both cases the events are observed well after maximum light.

(A color version of this figure is available in the online journal.)

are brighter than expected for a supernova, but are consistent with the presence of the NLS1. These detections are below the threshold of past radio surveys like FIRST and are therefore consistent with no change occurring due to CSS100217. The lack of detection in *Fermi* data does not place a strong constraint on the nature of this event as the follow-up spectra are not consistent with broad-line Type Ib/c supernovae that have been linked to GRBs. Type IIn supernova such as 2006gy have been detected in X-rays (Smith et al. 2007) but once again the detection of CSS100217 by *Swift* is consistent with emission from the NLS1.

Massive η Carinae-like LBVs undergo large outbursts and deposit material into the interstellar medium that will eventually be illuminated when the stars explode. In these cases much of the kinetic energy of these explosions is converted to luminosity. The brightness limit of such events is mainly constrained by the amount and distribution of circumstellar material interacting with the supernova shock. A series of dense circumstellar shells or a surrounding dense medium can give rise to extreme luminosity so that the explosion appears like a supermassive star. Although the optical energy expended by the event is higher than any past Type IIn supernova, it is within a factor of three of the bolometric values for SN 2006gy (5×10^{51} erg; Smith et al. 2010a) and SN 2003ma (4×10^{51} erg; Rest et al. 2011). The presence of strong continuum evolution and ongoing strong Balmer emission, along with a bright and distinctly supernova-like light curve, suggests that CSS100217 is most likely an extremely luminous Type IIn supernova near the nucleus of an AGN/starburst galaxy. Further photometric and spectroscopic monitoring of CSS100217 should secure the nature of this event and also give further insight into the nature of the host galaxy.

5.4. A Supernova Associated with the AGN?

A key piece of evidence is the observed proximity of the transient to the AGN of the host, since both the *HST* and

the Keck AO observations indicate a single, unresolved point source, consistent with a single PSF. It is worth noting that they span a range of ∼5–6 in wavelength, so that the absence of a second point source in either one cannot be attributed to a hypothetical extreme difference in colors. For the *HST*, Sparrow's resolution limit is 0.″043. The resolution of the Keck AO images is comparable, with 0.04 arcsec pixels. Using the *HST* resolution limit and the distance to CSS100217 based on the redshift, we find that CSS100217 occurred within ∼150 pc of the galactic nucleus.

The probability of a chance alignment seems small, although it cannot be rigorously excluded. Since NLS1 are expected to largely occur in spiral galaxies (Crenshaw et al. 2003), with typical half-light radii of a few kpc, the possibility of a chance alignment along the line of sight but far from the AGN is a priori very small, depending on the unknown central density profile of the host. We also note that there is no evidence for a redshift offset between the AGN emission and the event emission. Since the narrow-line region in Seyfert 1 galaxies have been measured to extend to sizes from 700 pc to 1.5 kpc (Bennert et al. 2006), the event likely occurred well within the limits of the narrow-line region.

Significant star formation has been indicated within the nuclear regions of number of Seyfert 1 galaxies and nuclear starbursts have been predicted in the dusty tori of Seyfert galaxies (Imanishi & Wada 2004; Riffel et al. 2007). The presence of rapid star formation would naturally lead to Type II supernovae in such regions. However, there is no morphological evidence of star-forming regions or superposed dust lanes outside of the nucleus, and again, the broad range of wavelengths (*U* to *K* bands) as well as the lack of any reddening signature in our spectra argue against it being hidden by dust. This suggests that any star-forming activity is likely within the region dominated by the AGN, rather than in some unrelated region in its vicinity.

On the other hand, a strong *UVX* radiation field in the vicinity of the AGN would preclude star formation, unless it is well shielded. One interesting possibility is that the event is a supernova associated with the outer edges of the accretion disk, where it would be shielded from the AGN radiation. These outer regions of the accretion disks are expected to be violently unstable, naturally leading to fragmentation and star formation, as predicted originally by Shlosman & Begelman (1987, 1989), and further fortified by the modern numerical and semi-analytical models (Goodman 2003; Goodman & Tan 2004; Jiang & Goodman 2011). Moreover, these models favor the formation of very massive stars, which would fit naturally with the event as a hyperluminous supernova. If so, this would be the first detection of such a supernova from an AGN accretion disk.

A question naturally arises, why such events have not been reported previously, either by us or by other groups? A likely cause is the deliberate bias of supernova searches against AGNs, where any observed variability could be naturally assumed to be associated with the AGN itself. With sufficient sampling transient surveys can now build empirical models of nuclear optical variability. This allows us to separate the slowly changing variability occurring over long timescales, common in AGNs, from the rapid changes seen due to TDEs and supernovae. As we have shown above, CSS100217 is highly unlikely to be an instance of a normal AGN variability. The use of aperture photometry in the CRTS survey produces bias against detecting optical transients such as regular supernovae in the brightest regions of intrinsically luminous galaxies (Drake et al. 2009). For this reason only events brighter than $M_{V_{\rm CSS}} \sim -21$ would have been detected in this particular host galaxy. However, an event as luminous as CSS100217 would be detected at any location within almost any galaxy to the distance of CSS100217. We will report on a systematic search for more such events in the CRTS data in a forthcoming paper.

We thank Minjin Kim for help in analyzing the SDSS spectrum. The CRTS survey is supported by the U.S. National Science Foundation under grants AST-0909182 and CNS-0540369. Support for program number GO proposal 12117 was provided by NASA through a grant from the Space Telescope Science Institute, which is operated by the Association of Universities for Research in Astronomy, Inc., under NASA contract NAS 5-26555. The work at Caltech was supported in part by the NASA *Fermi* grant 08-FERMI08-0025, and by the Ajax Foundation. The CSS survey is funded by the National Aeronautics and Space Administration under grant no. NNG05GF22G issued through the Science Mission Directorate Near-Earth Objects Observations Program. J.L.P. acknowledges support from NASA through Hubble Fellowship Grant HF-51261.01-A awarded by the STScI, which is operated by AURA, Inc. for NASA, under contract NAS 5-26555. The PQ survey is supported by the U.S. National Science Foundation under Grants AST-0407448 and AST-0407297. Support for M.C. is provided by Proyecto Basal PFB-06/2007, by FONDAP Centro de Astrofísica 15010003, and by MIDEPLAN Rs Programa Iniciativa Científica Milenio through grant P07-021-F, awarded to The Milky Way Millennium Nucleus. *GALEX* (*Galaxy Evolution Explorer*) is a NASA Small Explorer, launched in 2003 April. We gratefully acknowledge NASA's support for construction, operation, and science analysis for the *GALEX* mission, developed in cooperation with the Centre National d'Etudes Spatiales of France and the Korean Ministry of Science and Technology. The Expanded Very Large Array is operated by the National Radio Astronomy Observatory, a facility of the National Science Foundation operated under cooperative agreement by Associated Universities, Inc. We thank the staff of GMRT that made these observations possible. GMRT is run by the National Centre for Radio Astrophysics of the Tata Institute of Fundamental Research. The *Fermi* LAT Collaboration acknowledges support from a number of agencies and institutes for both the development and the operation of the LAT as well as scientific data analysis. These include NASA and DOE in the United States, CEA/Irfu and IN2P3/CNRS in France, ASI and INFN in Italy, MEXT, KEK, and JAXA in Japan, and the K. A. Wallenberg Foundation, the Swedish Research Council and the National Space Board in Sweden. We thank all the observers at ARIES who provided their valuable time and support for the observations of this event. The *UBVRI* observations presented here are included by R.R. in partial fulfillment of the requirements for a Ph.D. degree.

REFERENCES

Abadie, J., et al. 2010, ApJ, 715, 1453
Abazajian, K. N., et al. 2009, ApJS, 182, 543
Abdo, A. A., et al. 2009, ApJ, 706, L138
Abdo, A. A., et al. 2010a, ApJS, 188, 405
Abdo, A. A., et al. 2010b, ApJ, 715, 429
Adelman-McCarthy, J. K., et al. 2006, ApJS, 162, 38
Ai, Y. L., et al. 2010, ApJ, 716, 31
Akerlof, C., et al. 2000, AJ, 119, 1901
Alcock, C., et al. 2003, Nature, 365, 621

Anderson, J., & King, I. R. 2000, PASP, 112, 1360
Atwood, W. B., et al. 2009, ApJ, 697, 1071
Aubourg, E., et al. 1993, Nature, 365, 623
Baars, J. W. M., Genzel, R., Pauliny-Toth, I. I. K., & Witzel, A. 1977, A&A, 61, 99
Baldwin, J. A., Phillips, M. M., & Terlevich, R. 1981, PASP, 93, 5
Barthelmy, S. D., et al. 2005, Space Sci. Rev., 120, 143
Bauer, A., et al. 2009, ApJ, 699, 1732
Becker, R. H., White, R. L., & Helfand, D. J. 1995, ApJ, 450, 559
Bennert, N., et al. 2006, A&A, 459, 55
Bentz, M. C., Peterson, B. M., Netzer, H., Pogge, R. W., & Vestergaard, M. 2009, ApJ, 697, 160
Bessell, M. S., & Brett, J. M. 1988, PASP, 100, 1134
Binney, J., & Merrifield, M. 1998, in Galactic Astronomy, ed. J. P. Ostriker & D. N. Spergel (Princeton, NJ: Princeton Univ. Press), 53
Boller, R., Brandt, W. N., & Fink, H. 1996, A&A, 305, 53
Botticella, M. T., et al. 2008, A&A, 479, 49
Cappelluti, N., et al. 2009, A&A, 495, L9
Catelan, M., et al. 2009, CBET, 1780, 1
Chevalier, R. A., Fransson, C., & Nymark, T. K. 2006, ApJ, 641, 1029
Condon, J. J., et al. 1998, AJ, 115, 1963
Cooke, J., et al. 2010, ATel, 2491
Crenshaw, D. N., Kraemer, S. B., & Gabel, J. R. 2003, AJ, 126, 1690
Croft, S., et al. 2009, BAAS, 41, 402
Deo, R. P., Crenshaw, D. M., & Kraemer, S. B. 2006, AJ, 132, 321
Djorgovski, S. G., et al. 2008, Astron. Nachr., 329, 263
Djorgovski, S. G., et al. 2001a, in ESO Astrophysics Symposia, Mining the Sky, Exploration of Large Digital Sky Surveys, ed. A. J. Banday et al. (Berlin: Springer), 305
Djorgovski, S. G., et al. 2001b, Proc. SPIE, 4477, 43
Drake, A. J., et al. 2009, ApJ, 696, 870
Drake, A. J., et al. 2010a, ApJ, 718, L127
Drake, A. J., et al. 2010b, ATel, 2725
Drake, A. J., et al. 2010c, ATel, 2784
Esquej, P., et al. 2007, A&A, 462, L49
Fransson, C., et al. 2005, ApJ, 622, 991
Gal-Yam, A., et al. 2010, Nature, 465, 322
Gerardy, C. L., et al. 2002, ApJ, 575, 1007
Gezari, S., et al. 2009a, ApJ, 698, 1367
Gezari, S., et al. 2009b, ApJ, 690, 1313
Gezari, S., Forster, K., Neill, J. D., & Martin, D. C. 2010, ATel, 2554, 1
Goodman, J. 2003, MNRAS, 339, 937
Goodman, J., & Tan, J. 2004, ApJ, 608, 108
Hagen, H. J., Engels, D., & Reimers, D. 1997, A&A, 324, L29
Halpern, J. P., Leighly, K. M., & Marshall, H. L. 2003, ApJ, 585, 665
Hills, J. G. 1975, Nature, 254, 295
Ho, L. C., et al. 1997, ApJ, 487, 568
Hodapp, K. W., et al. 2004, Astron. Nachr., 325, 636
Imanishi, M., & Wada, K. 2004, ApJ, 617, 214
Ivezic, Z., et al. 2008, arXiv:0805.2366
Izotov, Y. I., Thuan, T. X., & Guseva, N. G. 2007, ApJ, 671, 1297
Jahoda, K., et al. 1996, Proc. SPIE, 2808, 59
Jester, S., Schnieder, D. P., & Richards, G. T. 2005, AJ, 130, 873
Jiang, Y.-F., & Goodman, J. 2011, ApJ, 730, 45
Johnston, S., et al. 2007, PASA, 24, 174
Kankare, E., et al. 2010, ATel, 2716
Kauffmann, G., et al. 2003, MNRAS, 346, 1055
Keller, S. C., et al. 2007, PASA, 24, 1
Kewley, L. J., Groves, B., Kauffmann, G., & Heckman, T. 2006, MNRAS, 372, 961
Kewley, L. J., et al. 2001, ApJ, 556, 121
Klebesadel, R. W., Strong, I. B., & Olson, R. A. 1973, ApJ, 182, L85
Komossa, S., Bohringer, H., & Huchra, J. P. 1999, A&A, 349, 88
Komossa, S., et al. 2002, in Lighthouses of the Universe: Proc. of the MPA/ESO/MPE/USM Joint Astronomy Conf., ed. M. Gilfanov, R. Sunyaev, & E. Churazov (Berlin: Springer-Verlag), 436
Komossa, S., et al. 2008, ApJ, 678, L13
Komossa, S., et al. 2009, ApJ, 701, 105
Kozlowski, S., et al. 2010, ApJ, 722, 1624
Landolt, A. U. 1992, AJ, 104, 372
Larson, S., et al. 2003, BAAS, 35, 982
Leighly, K., & Moore, J. R. 2004, ApJ, 611, 107
Li, W., et al. 2006, PASP, 118, 37
Liu, H., Wang, J., Mao, Y., & Wei, J. 2010, ApJ, 715, L113
Lodato, G., & Rossi, E. M. 2011, MNRAS, 410, 359
Magorrian, J., & Tremaine, S. 1999, MNRAS, 309, 447
Maksym, W. P., Ulmer, M. P., & Eracleous, M. 2010, ApJ, 722, 1035
Mao, Y., Wang, J., & Wei, J. 2009, ApJ, 698, 859
Martin, D. C., et al. 2005, ApJ, 619, L1
Mattila, S., Meikle, W. P. S., & Greimel, R. 2004, New Astron. Rev., 48, 595
Mauch, T., & Sadler, E. M. 2007, MNRAS, 375, 931
Miller, A. A., et al. 2009, ApJ, 690, 1303
Monet, D., et al. 2003, AJ, 125, 984
Nakar, E., Piran, T., & Granot, J. 2002, ApJ, 579, 699
Nelson, C. A., et al. 2009, arXiv:0902.2213
Osterbrock, D. E., & Pogge, R. W. 1985, ApJ, 297, 166
Paczynski, B. 1986, ApJ, 304, 1
Paczynski, B. 1997, arXiv:atro-ph/9712123
Paczynski, B. 2000, PASP, 112, 1281
Perez-Torres, M. A., et al. 2007, ApJ, 671, L21
Perez-Torres, M. A., et al. 2010, arXiv:1008.4466
Quimby, R. M., et al. 2006, CBET, 644, 1
Rau, A., et al. 2009, PASP, 121, 1334
Rengelink, R. B., et al. 1997, A&AS, 124, 259
Rest, A., et al. 2011, ApJ, 729, 88
Richardson, D., Branch, D., Casebeer, D., Millard, J., Thomas, R. C., & Baron, E. 2002, AJ, 123, 745
Riffel, R., Pastoriza, M. G., Rodriguez-Ardila, A., & Maraston, C. 2007, ApJ, 659, 103
Rottgering, H. J. A. 2003, New Astron. Rev., 47, 405
Schawinski, K., et al. 2008, Science, 321, 223
Schlegel, D., et al. 1998, ApJ, 500, 525
Sesar, B., et al. 2007, AJ, 134, 2236 (The SDSS team)
Shlosman, I., & Begelman, M. 1987, Nature, 329, 810
Shlosman, I., & Begelman, M. 1989, ApJ, 341, 685
Skrutskie, M. F., et al. 2006, AJ, 131, 1163
Smith, N., et al. 2007, ApJ, 666, 1116
Smith, N., et al. 2010a, ApJ, 709, 856
Smith, N., et al. 2010b, AJ, 139, 1451
Soderberg, A. M., et al. 2008, Nature, 453, 469
Stanek, K. Z., et al. 2003, ApJ, 591, L17
Stasinska, G., et al. 2006, MNRAS, 371, 972
Stetson, P. B. 1987, PASP, 99, 191
Strubbe, L. E., & Quataert, E. 2009, MNRAS, 400, 2070
Strubbe, L. E., & Quataert, E. 2010, arXiv:1008.4131
Tomaney, A. B., & Crotts, A. P. S. 1996, AJ, 112, 2872
Terlevich, R., Tenorio-Tagle, G., Franco, J., & Melnick, J. 1992, MNRAS, 255, 713
Trundle, C., et al. 2009, A&A, 504, 945
Turatto, M., Cappellaro, E., Danziger, I. J., Benetti, S., Gouiffes, C., & della Valle, M. 1993, MNRAS, 262, 128
Ueno, S., et al. 2008, Proc. SPIE, 7011, 75
Ulrich, M.-H., Maraschi, L., & Urry, C. M. 1997, ARA&A, 35, 445
Ulvestad, J. S., & Ho, L. C. 2001, ApJ, 558, 561
Valenti, S., et al. 2010, ATel, 2773
van Velzen, S., et al. 2010, arXiv:1009.1627
Véron-Cetty, M.-P., & Véron, P. 2010, A&A, 518, 10
Wang, J., & Merritt, D. 2004, ApJ, 600, 149
Webb, W., & Malkan, M. 2000, ApJ, 540, 652
Wizinowich, P., et al. 2006, PASP, 118, 297
Yuan, W., Zhou, H. Y., Komossa, S., Dong, X. B., Wang, T. G., Lu, H. L., & Bai, J. M. 2008, ApJ, 685, 801
Zhao, F. Y., Strom, R. G., & Jiang, S. Y. 2006, Chin. J. Astron. Astrophys., 6, 635
Zhou, H.-Y., Wang, T.-G., Dong, X.-B., Zhou, Y.-Y., & Li, C. 2003, ApJ, 584, 147
Zhou, H. Y., et al. 2006, ApJS, 166, 128